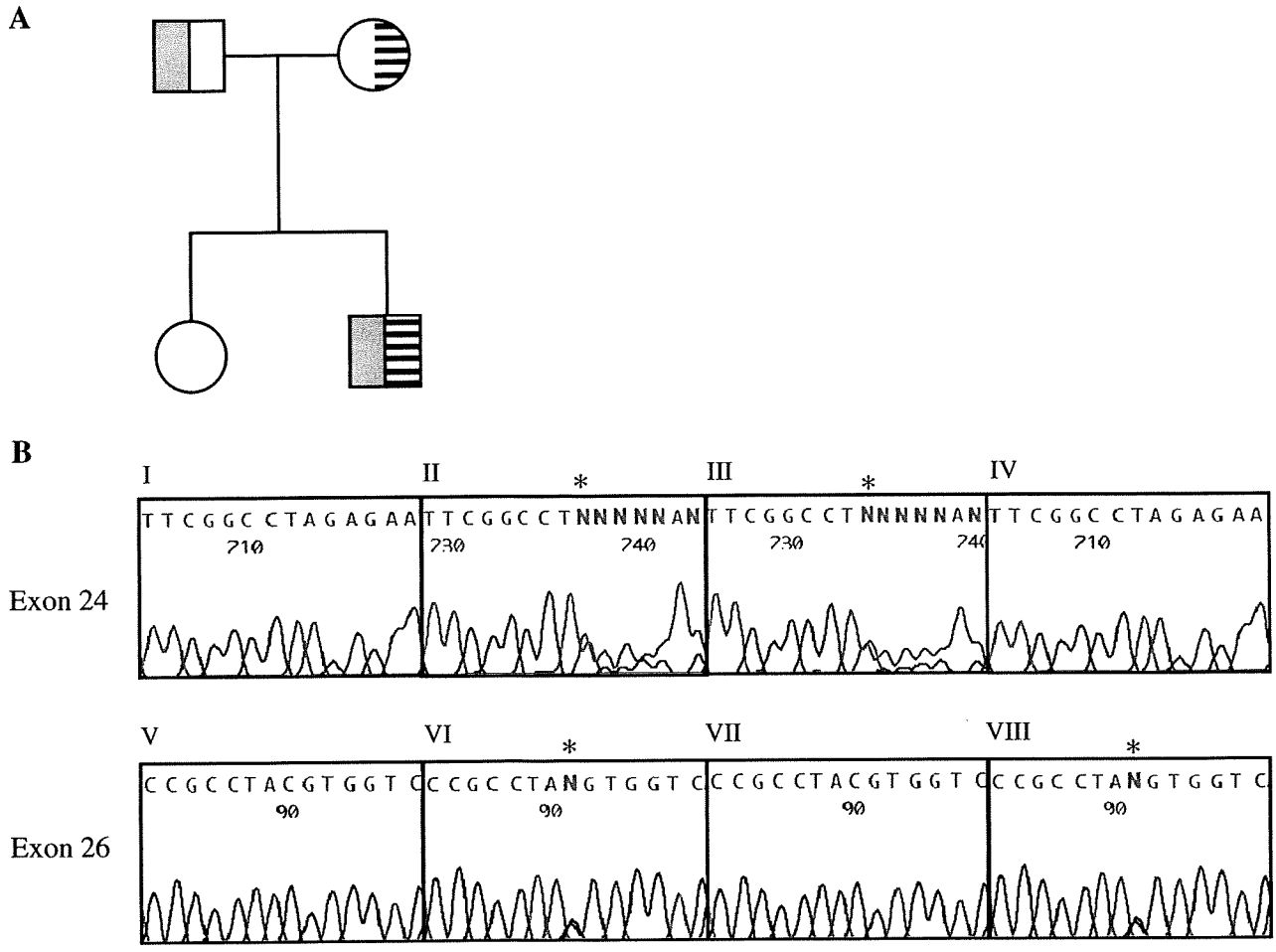

Fig. 1. (A) Pedigree of the family with C3 deficiency in this study. The patient was revealed to have compound heterozygous *C3* gene mutations with a paternal mutation (indicated as dark shadings) and a maternal mutation (indicated as horizontal strips). (B) Sequencing analysis of the patient with C3 deficiency and his family members I–IV: Sequence of a portion of exon 24 in the *C3* gene; normal individual (I), patient (II), patient's father (III) and patient's mother (IV). The mutation, derived from his father (indicated as dark shading in A) is a 1-bp insertion (3176insT) (asterisk mark indicates insertion point). V–VIII: Sequence of a portion of exon 26 in the *C3* gene; normal individual (V), patient (VI), patient's father (VII) and patient's mother (VIII). The mutation derived from his mother (indicated as horizontal strips in A) is a nonsense mutation described as C3303G (Y1081X) (asterisk mark indicates the mutated nucleotide).

affecting the different chains, can be compensated for by binding of the remaining wild type and the functionally normal α and β chains from the different alleles to avoid a more severe C3 deficiency. This hypothesis seemed consistent with the unexpected findings in hereditary C3 deficiency; its extremely rare occurrence and high ratio of homozygous mutation occurrence.

Case report

The pedigree of C3 deficiency is shown in Fig. 1A. The patient is a 2-year-old Japanese boy, who had suffered from several bacterial infections, such as meningitis, bronchitis and pneumonia. His parents and 5-year-old sister were all in good health. The parents were not related. Laboratory findings of the patient at this time were as follows: undetectable serum C3 level (<2 mg/dl; normal range, 75–150 mg/dl) and low CH50 (<12 U/ml; normal range, 35–45 U/ml). Blood examination of family members revealed that their serum C3 levels were 46 mg/dl in the father, 51 mg/dl in the mother and normal level in the sister, respectively. Serum CH50 levels were 33 U/ml in the father and 23 U/ml in the mother. Serum C4 levels in these family members were all within the normal range.

Materials and methods

Informed consent was obtained from his parents. Genomic DNA from family members, as well as from control individuals, was PCR-amplified for over the entire coding sequence of the *C3* gene including all its exon–intron boundaries using appropriate primers. PCR amplification products were purified using a QIAEX II Gel Extraction Kit (Qiagen) and directly sequenced in both directions using ABI PRISM 310 Genetic Analyzer (Applied Biosystems, Foster City, CA, USA).

Results and discussion

The patient was shown to have compound heterozygous *C3* gene mutations as shown in the Fig. 1B. They were a novel one base insertion (3176insT) in exon 24 which is predicted to result

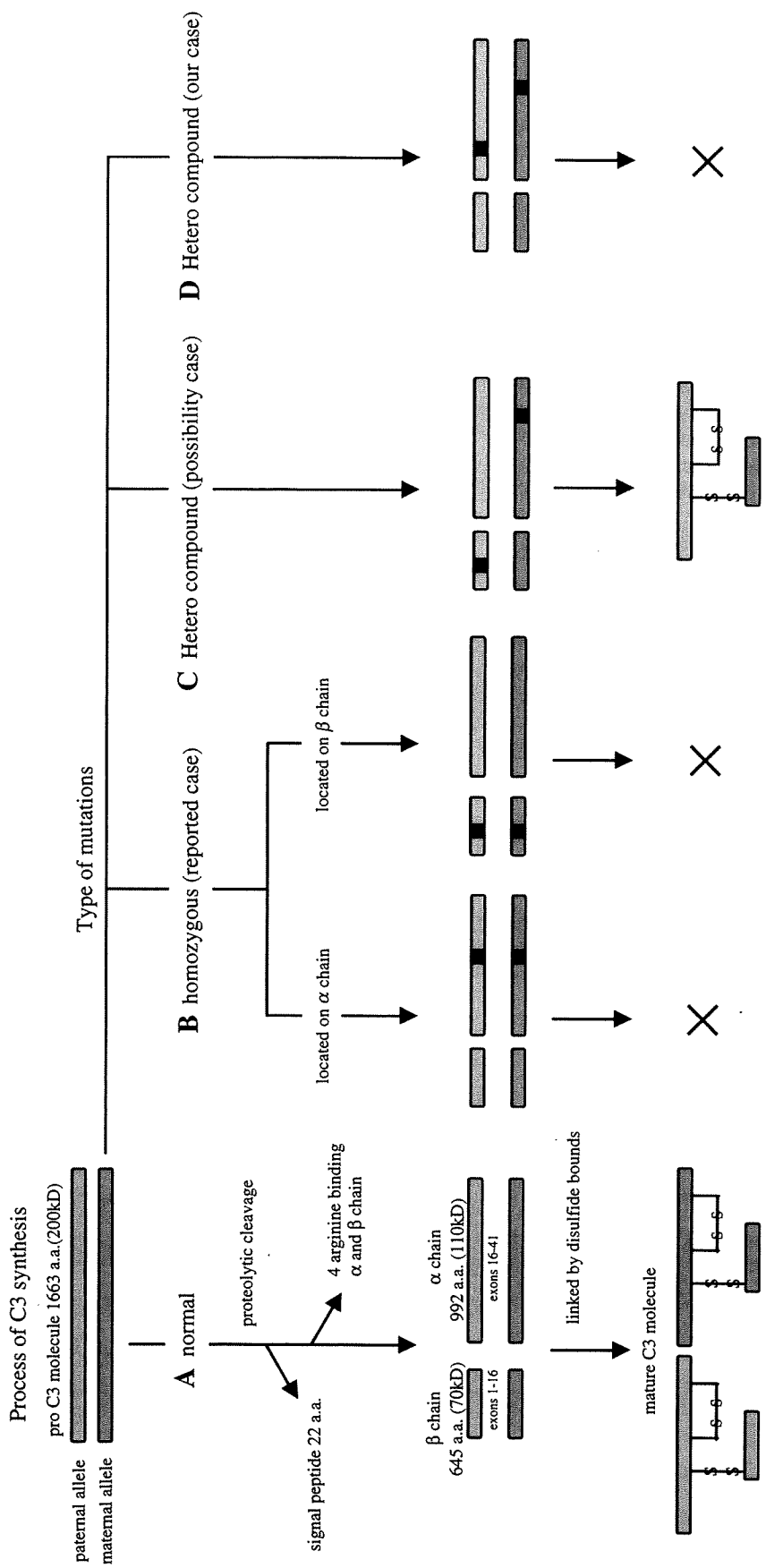

Fig. 2. The proposed hypothesis with regard to the mechanism of C3 deficiency based on the unique process of C3 synthesis. (A) Normal synthesis of the mature C3 molecule. (B–D) Various combinations of the *C3* gene mutations. (B) Homozygous mutations in the *C3* gene. No functional mature C3 molecule can be produced because both mutations ruin the same chains. (C) Hypothetical case: in some combinations of mutations in the different allele, a mature C3 molecule could be produced from functional α and β chains from the different allele. (D) Our case with compound heterozygous *C3* gene mutations. In both the mutations located in the same C3 α chain, no functional C3 molecule can be produced.

in a frameshift and a premature downstream stop codon (K1105X) in exon 26, and a nonsense mutation of C3303G (Y1081X) in exon 26, which was previously reported as homozygous mutations elsewhere [7]. These defects were not found in any unaffected family members or in 100 healthy control individuals. Both patient's PCR fragments (exon 24 and exon 26) were ligated to pCR2.1 TA cloning vector (Invitrogen, Carlsbad, CA, USA) and transformed INVαF′ (Invitrogen, Carlsbad, CA, USA) competent cells for confirming the mutant clone sequence. It is noted that both the mutations are predicted to result in a truncation of the α chain of the C3 molecule. This finding may be linked to the unique process of C3 synthesis. The *C3* mRNA is translated into a signal peptide precursor form of pro-C3 molecule from each allele (paternal and maternal alleles), and subsequently processed by proteolytic cleavage into the β chain (13 kb from exons 1–16) and the α chain (28 kb from exons 16–41) [10], which are cross-linked by disulfide bonds to make the mature C3 molecule (Fig. 2A). Almost all cases with C3 deficiency have been reported as homozygous mutations in the *C3* gene. No functional mature C3 molecule can be produced (Fig. 2B). The hypothesis: a possible case without C3 deficiency in spite of harboring compound heterozygous *C3* gene mutations. The functional α and β chains from the different allele can be recombined to avoid severe deficiency (Fig. 2C) with the exception of nonsense mutation in β chain, in this case neither the functional α nor β chains could be synthesized from one allele with nonsense mutation. Although our case is an exceptional one with compound heterozygous *C3* gene mutations, no functional C3 can be produced (Fig. 2D). Thus, although this is the first exceptional case with heterozygous *C3* gene mutations confirmed, it is still consistent with our hypothesis. Moreover, though there might be a patient having gene mutations such as Fig. 2C, he or she avoids severe deficiency for existence of the functional α and β chains, as a result it might not be detected as C3 deficiency. The reason why the C3 deficiency is an extremely rare disease and for the high ratio of homozygous mutation occurrence might be based on such backgrounds. Further studies, for more cases with C3 deficiency that have been characterized at the molecular level, will be needed to confirm this hypothesis.

References

[1] M. Botto, K.Y. Fong, A.K. So, A. Rudge, M.J. Walport, Molecular basis of hereditary C3 deficiency, J. Clin. Invest. 86 (1990) 1158–1163.
[2] M. Botto, K.Y. Fong, A.K. So, R. Barlow, R. Routier, B.J. Morley, M.J. Walport, Homozygous hereditary C3 deficiency due to a partial gene deletion, Proc. Natl. Acad. Sci. U. S. A. 89 (1992) 4957–4961.
[3] H. Fujioka, T. Ariga, M. Yoda, M. Ohsaki, K. Horiuchi, M. Otsu, T. Sugihara, Y. Sakiyama, A case of C3 deficiency with a novel homozygous two-base deletion in the C3 gene, Am. J. Med. Genet. A 138 (2005) 399–400.
[4] J.L. Huang, C.Y. Lin, A hereditary C3 deficiency due to aberrant splicing of exon 10, Clin. Immunol. Immunopathol. 73 (1994) 267–273.
[5] L. Singer, W.T. Whitehead, H. Akama, Y. Katz, Z. Fishelson, R.A. Wetsel, Inherited human complement C3 deficiency. An amino acid substitution in the beta-chain (ASP549 to ASN) impairs C3 secretion, J. Biol. Chem. 269 (1994) 28494–28499.
[6] H. Tsukamoto, T. Horiuchi, H. Nishizaka, T. Sawabe, S. Harashima, C. Morita, Y. Kashiwagi, K. Masumoto, D. Himeji, E. Kitano, H. Kitamura, Y. Jinpo, Molecular analysis of human complement C3 deficiency with systemic lupus erythematosus, Jpn. J. Rheumatol. 40 (2000) 418 (in Japanese).
[7] W. Matsuyama, M. Nakagawa, H. Takashima, F. Muranaga, Y. Sano, M. Osame, Molecular analysis of hereditary deficiency of the third component of complement (C3) in two sisters, Intern. Med. 40 (2001) 1254–1258.
[8] E. Da Silva Reis, G.V. Baracho, A. Sousa Lima, C.S. Farah, L. Isaac, Homozygous hereditary C3 deficiency due to a premature stop codon, J. Clin. Immunol. 22 (2002) 321–330.
[9] M.H. de Bruijn, G.H. Fey, Human complement component C3 cDNA cording sequence and derived primary structure, Proc. Natl. Acad. Sci. 82 (1985) 708–712.
[10] K.Y. Fong, M. Botto, M.J. Walport, A.K. So, Genomic organization of human complement component C3, Genomics 7 (1990) 579–586.

The Clinical Feature of Invasive Fungal Infection in Pediatric Patients With Hematologic and Malignant Diseases

A 10-year Analysis at a Single Institution at Japan

Ryoji Kobayashi, MD, PhD,† Makoto Kaneda, MD,† Tomonobu Sato, MD, PhD,*† Mizuho Ichikawa, MD,† Daisuke Suzuki, MD,† and Tadashi Ariga, MD, PhD†*

Summary: Invasive fungal infections (IFI) are an important complication in hematologic malignancies and stem-cell transplantation (SCT). However, there are limited data characterizing IFI in children. The clinical feature of IFI after chemotherapy and SCT were analyzed in 334 pediatric patients treated at Hokkaido University Hospital from 1997 to 2006. The cumulative incidence of IFI was 6.9%; this comprised cases of proven, probable and possible IFI at rates of 1.2%, 3.0%, and 2.7%, respectively. The infected lesions were lung in 14 patients, liver in 5 patients, brain in 3 patients, fungemia in 2 patients, kidney in 1 patient, and endophthalmitis in 1 patient. The mortality of IFI was 48.2%, excluding patients who died due to relapse and interstitial pneumonitis; in particular, 71.4% patients with a lung lesion (10/14) died due to IFI. Fifty-nine pediatric patients died in our institution over the 10-year period of the study and IFI was the direct cause of death in 18.6% (11/59) of the patients. Risk factors for IFI with chemotherapy and SCT were also analyzed. Univariate analysis showed that age at diagnosis older than 10 years, relapse of original disease, long-term administration of broad-spectrum antibiotics, and acute myelogenous leukemia (AML) were the risk factors for IFI. All patients with IFI received long-term antibiotic therapy. AML was most strongly associated using a multivariate analysis. The prognosis of IFI has been expected poor; therefore, prevention of this condition, especially for older patients with AML, would be important.

Key Words: invasive fungal infection, AML, hematologic malignancy

(*J Pediatr Hematol Oncol* 2008;30:886–890)

There has been a drastic improvement in the field of treatment for pediatric patients with hematologic and malignant disorders. The survival rate of patients with pediatric leukemia and malignant tumor has improved due to development of multidrug chemotherapy. Immunosuppressive therapy with antithymocyte globulin and cyclosporine is the most common treatment for aplastic anemia and the response rate to this treatment in newly diagnosed severe aplastic anemia is 60% to 80%.[1,2] In addition, stem-cell transplantation (SCT) has improved survival rates in patients with hematologic disorders, malignant disorders, immunodeficiencies, and metabolic disorders. On the other hand, the introduction of more intensive treatment has been accompanied by the increasing rate of invasive fungal infection (IFI). IFI in patients with hematologic and malignant diseases has become a problem for several decades and is now a significant cause of morbidity and mortality in such patients. As diagnosis of IFI is difficult, the presence of fungal infection is frequently discovered only at autopsy.[3] Despite advances in nonculture-based procedures, such as the introduction of the galactomannan antigen enzyme-linked immunosorbent assay and polymerase chain reaction tests for fungal DNA, timely diagnosis of IFI in SCT patients still remains difficult.[4,5]

There are limited data characterizing IFI in children.[6–11] Therefore, to determine the incidence, risk factors, and mortality for IFI, we analyzed IFI in pediatric patients with hematologic malignancies, aplastic anemia, solid tumor, and other nonmalignant diseases who received chemotherapy, immunosuppressive treatment, and SCT in a single center in Japan.

PATIENTS AND METHODS

Patients

A total of 334 pediatric patients with different hematologic malignancies, aplastic anemia, solid tumor, metabolic abnormalities, and immunodeficiencies received chemotherapy, immunosuppressive therapy, and SCT in Hokkaido university hospital between January 1997 and December 2006. Of these patients, 198 were boys and 136 were girls. Data were analyzed for 524 admissions. The age at admission ranged from 10 days to 29 years old (median: 5.4 y old). Ninety-nine patients had acute lymphoblastic leukemia, 51 had acute myelogenous

Received for publication April 7, 2008; accepted July 3, 2008.
From the *Department of Pediatrics, Sapporo Hokuyu Hospital; and †Department of Pediatrics, Hokkaido University Graduate School of Medicine, Sapporo, Japan.
Reprints: Ryoji Kobayashi, MD, PhD, Department of Pediatrics, Sapporo Hokuyu Hospital, Higashi-Sapporo 6-6, Shiroishiku Sapporo, 003-0006, Japan (e-mail: r-koba@jacls.jp).

leukemia (AML), 40 had aplastic anemia, 29 had neuroblastoma, 17 had Wilms tumor; 86 had other malignant diseases, and 12 had nonmalignant diseases, including 8 with immunodeficiency and 4 with metabolic disease who were admitted for SCT. During the study period, 135 patients received SCT: 14 received autologous SCT and 121 received allogeneic SCT. The origin of the stem cells was as follows: 82 patients received bone marrow transplantation (BMT), 9 underwent peripheral blood SCT (PBSCT), and 44 received cord blood SCT (CBSCT). Data were analyzed as of January 1, 2007. Galactomannan test was performed when there was a clinical suspicion of IFI. This is same in cases of chemotherapy and SCT. Rate of autopsies was 9 out of 59 dead episodes (15.3%).

Definition of IFI

We identified patients who developed proven, probable, or possible IFI using standardized definitions set forth by the European Organization for Research and Treatment of Cancer and the National Institute of Allergy and Infectious Diseases Mycoses Study Group.[12]

Infection Prophylaxis

An inpatient ward was built at our hospital in 1994, with basic 4-person rooms and 11 private rooms. A private room was used for induction therapy for leukemia. Moreover, an aseptic bed using a high-efficiency particulate air filter was used for treatment involving bone marrow suppression. SCTs were performed in a clean room of NASA class 100. Construction in the ward was performed 2 times during the study period: the conference room was increased in size in 2003 and the clean room was moved in 2006. Trimethoprim-sulfamethoxazole was used in all patients for prevention of *Pneumocystis carinii* pneumonia. Before March 2006, prophylactic administration of oral amphotericin B 50 mg/kg/d was used as an antifungal drug for all patients receiving chemotherapy. After April 2006, oral fluconazole 10 mg/kg/d was administered as prophylaxis for fungal infection. Before March 2005, amphotericin B 100 mg/kg/d was used before SCT, but after April 2005 intravenous micafungin 1 mg/kg/d was introduced from the start of the conditioning regimen until neutrophil recovery, followed by oral fluconazole 10 mg/kg from after neutrophil recovery until the date of discharge.

Statistical Analysis

A t test or χ^2 test was used to compare patients who did and did not develop IFI. Analysis of mortality was performed using the Kaplan-Meier method, with differences compared by log-rank test. Stepwise multivariate regression analysis was performed to explore the independent effect of variables that showed a significant effect in univariate analysis. Statistical analyses were performed using SPSS II for Windows (release 11.0.1J, SPSS Japan Inc).

RESULTS

Incidence of IFI

The cumulative incidence of IFI in this study was 6.9% (23/334) (Table 1). The 23 cases comprised 4 of proven IFI (4/334: 1.2%), 10 of probable IFI (10/334: 3.0%), and 9 of possible IFI (9/334: 2.7%). IFI occurred in 11 patients with AML and 11 patients with a history of SCT. The infected lesions were lung in 14 patients, liver in 5 patients, brain in 3 patients, fungemia in 2 patients, kidney in 1 patient, and endophthalmitis in 1 patient. *Candida albicans* (patient 15) and *Candida krusei* (patient 21), respectively, were detected in the blood culture of the patients with fungemia. In patients with proven IFI, hyphae were detected by pulmonary histopathologic examination on necropsy in 1 patient (patient 8) and detected in a brain abscess in another patient (patient 22). In the 5 patients with probable IFI, galactomannan antigen was detected in blood samples. The number of hospitalizations every year according to disease and the number of cases of IFI are shown in Table 2. After 2004, 16 patients developed IFI, which accounted for 69.5% of the total number of cases. Two patients were thought to have breakthrough infection. One patient was case 21. She was administered fluconazole as prophylaxis. However, she had fungemia with *Candida krusei*. Another patient was case 22. She had been taken voriconazole as prophylaxis. However, she had lesion by *Mucor*.

Risk Factors for IFI

Univariate analysis showed that age at diagnosis more than 10 years old, relapse of original disease, long-term administration of broad-spectrum antibiotics, and AML were risk factors for IFI with chemotherapy and SCT (Table 3). In patients with IFI, the median age at diagnosis was significantly higher than that of patients who did not develop IFI; most patients with IFI were over 10 years old. The median age at diagnosis was 12.1 years old in patients with IFI, and the median age at onset of IFI was 14 years old. All patients with IFI received long-term antibiotic therapy and this factor was most associated with IFI. However, excluding this factor, AML was most strongly associated with IFI in a multivariate analysis (Table 4).

Outcome After IFI

Regarding antifungal drugs, micafungin, fluconazole, voriconazole, amphotericin B, itraconazole, miconazole, liposomal amphotericin B, and 5-fluorouracil were administered to 16, 13, 8, 7, 6, 3, 2, and 1 patients, respectively. Used terms of antifungal drugs were from 3 days to 14 months. However, antifungal therapy was effective in only 12 of the 23 patients with IFI. Seven of these 12 patients are still alive, but the other patients died after relapse and nonfungal interstitial pneumonitis (IP). Used term of antifungal drugs was not associated with prognosis. The mortality of IFI was 48.2%, excluding patients with relapse and IP, and was especially high in the 14 patients with a lung lesion: 71.4% (10/14) of these

TABLE 1. Clinical Characteristics and Outcomes for 23 Patients Who Developed IFI

	Age	Sex	Disease	SCT	Timing of IFI	Lesion	Definition	Suspected Pathogen	Treatment	Outcome	Survival Time (mo)
1	13	M	AML second CR	+	cGVHD (U-BMT)	Lung	Possible	-	FCZ, ITCZ	Survival	97+
2	5	M	AML relapse	–	Reinduction	Endophthalmitis	Possible	-	FCZ, MCZ	Death (relapse)	9
3	16	M	MDS (RA)	+	cGVHD (U-BMT)	Lung	Possible	-	FCZ, AMPH	Death (IFI)	0.1
4	14	F	EB-LPD (CID)	–	Induction	Lung	Possible	-	FCZ, AMPH	Death (IFI)	1
5	8	F	AML second CR	+	aGVHD (U-CBSCT)	Lung	Possible	-	FCZ, AMPH, ITCZ	Death (relapse)	78
6	3	F	AML relapse	+	Reinduction	Lung	Probable	*Aspergillus*	FCZ, MCZ, ITCZ	Death (IFI)	1
7	16	F	ALL second CR	+	Rejection (U-BMT)	Lung	Probable	*Aspergillus*	FCZ, MCFG, AMPH, ITCZ	Death (IFI)	1.5
8	18	M	SAA	+	Rejection (R-BMT)	Lung, brain	Proven	*Aspergillus*	FCZ, MCFG, AMPH, 5FC	Death (IFI)	1.5
9	17	F	ALL relapse	+	Reinduction	Lung	Probable	*Aspergillus*	FCZ, MCFG	Death (IFI)	2
10	17	M	AML first CR	+	cGVHD (U-BMT)	Lung	Probable	*Aspergillus*	FCZ, MCFG, ITCZ, AMPH	Death (IFI)	3
11	14	F	CAEBV	+	cGVHD (U-CBSCT)	Liver	Probable	-	FCZ, ITCZ	Survival	26+
12	14	M	AML first CR	–	Consolidation	Liver	Probable	-	FCZ, MCFG	Death (relapse)	12
13	4	M	ALL	–	Induction	Liver	Probable	-	FCZ, MCFG, AMPH	Death (IP)	16
14	0	M	X-SCID	–	On admission	Lung	Possible	*Aspergillus*	MCFG	Survival	34+
15	8	M	NB	–	Consolidation	Fungemia	Proven	*Candida albicans*	MCFG	Survival	13+
16	9	F	AML first CR	–	Consolidation	Liver	Probable	-	MCFG, VCZ	Survival	14+
17	15	F	AML relapse	–	Reinduction	Lung	Probable	*Aspergillus*	MCFG, VCZ	Death (IFI)	2
18	16	M	AML first CR	–	Consolidation	Kidney	Possible	-	MCFG, VCZ	Survival	11+
19	16	M	AML relapse	+	Reinduction	Lung	Possible	-	MCFG, VCZ	Death (IFI)	1.5
20	14	M	NK/T leukemia relapse	+	Reinduction	Liver, brain	Probable	-	MCFG, VCZ, MCZ	Death (IFI)	0.2
21	11	F	Ewing sarcoma	–	Consolidation	Fungemia	Proven	*Candida krusei*	MCFG, VCZ	Death (relapse)	2
22	8	F	AML first CR	–	Consolidation	Lung, brain	Proven	*Mucor*	MCFG, VCZ, lipoAMPH	Survival	3+
23	14	M	ALL relapse	–	Reinduction	Lung	Possible	-	MCFG, VCZ, lipoAMPH	Death (IFI)	1

aGVHD indicates acute graft-versus-host disease; ALL, acute lymphoblastic leukemia; AML, acute myelogenous leukemia; AMPH, amphotericin B; CAEBV, chronic active EB virus infection; cGVHD, chronic graft-versus-host disease; CID, congenital immunodeficiency; CR, complete remission; EB-LPD, EB virus-associated lymphoproliferative disease; FCZ, fluconazole; IFI, invasive fungal infection; IP, interstitial pneumonitis; ITCZ, itraconazole; lipoAMPH, liposomal amphotericin B; MCFG, micafungin; MCZ, miconazole; MDS, myelodysplastic syndrome; NB, neuroblastoma; NK, natural killer; RA, refractory anemia; R-BMT, related bone marrow transplantation; SAA, severe aplastic anemia; U-BMT, unrelated bone marrow transplantation; U-CBSCT, unrelated cord blood stem-cell transplantation; VCZ, voriconazole; X-SCID, X-linked severe combined immunodeficiency; 5FC, flucytosine.

TABLE 2. Number of Newly Diagnosed Inpatients According to Disease

	ALL	AML	AA	NB	Wilms Tumor	Other Malignancy	Nonmalignancy	Total	SCT	IFI
1996	5 (5)	4 (4)	3 (3)	0 (0)	0 (0)	3 (3)	0 (0)	15 (15)	0	0
1997	7 (11)	6 (7)	4 (6)	3 (4)	1 (2)	8 (10)	0 (0)	29 (40)	13	1
1998	2 (11)	7 (8)	4 (7)	1 (2)	1 (2)	8 (10)	2 (2)	25 (42)	9	0
1999	7 (7)	5 (6)	3 (4)	0 (1)	2 (3)	8 (13)	1 (1)	26 (35)	13	3
2000	11 (13)	0 (1)	6 (9)	4 (6)	2 (5)	6 (8)	0 (0)	29 (42)	11	1
2001	14 (21)	2 (3)	4 (6)	1 (1)	1 (2)	11 (15)	1 (1)	34 (49)	13	0
2002	10 (17)	7 (7)	4 (7)	4 (6)	2 (4)	7 (15)	1 (2)	35 (58)	13	3
2003	10 (22)	6 (8)	0 (0)	5 (11)	1 (2)	8 (9)	1 (1)	31 (53)	10	0
2004	11 (17)	5 (9)	5 (6)	5 (11)	3 (3)	7 (13)	3 (4)	39 (63)	16	6
2005	10 (19)	6 (11)	3 (3)	4 (11)	1 (3)	5 (15)	1 (1)	30 (63)	17	4
2006	12 (18)	3 (4)	4 (4)	2 (5)	3 (9)	15 (22)	2 (2)	41 (64)	20	5
Total	99 (161)	51 (68)	40 (55)	29 (58)	17 (35)	86 (133)	12 (14)	334 (524)	135	23

The total number of inpatients is shown in parentheses.
AA indicates aplastic anemia; ALL, acute lymphoblastic leukemia; AML, acute myelogenous leukemia; IFI, invasive fungal infection; NB, neuroblastoma; SCT, stem cell transplantation.

patients died due to IFI. Fifty-nine pediatric patients died in our institution over 10 years of the study period and IFI was the direct cause of death in 18.6% (11/59) of these patients.

DISCUSSION

Here, we reveal the clinical feature of IFI in pediatric patients with hematologic and malignant diseases in a single center in Japan. Our results show that the cumulative incidence of proven, probable, or possible IFI in pediatric patients undergoing chemotherapy, immunosuppressive therapy, and SCT was 6.9%, and the rate of proven and probable IFI was 4.2%. Rosen et al[11] reported the incidence of IFI in pediatric oncology patients to be 4.9%, with a rise in this incidence of 0.89% per year, giving the rate of 7.8% in 2001. We found a similar year-by-year increase in IFI in our hospital. This would be related to increasing treatment intensity and the development of diagnostic procedures such as serologic diagnosis, which allows increasingly accurate assessment of the cause of disease. We introduced prophylactic intravenous micafungin after April 2005 in patients with SCT, and fluconazole as prophylaxis after April 2006. However, no patient who was administered micafungin as prophylaxis in transplantation, had IFI.[13]

All patients with IFI received long-term broad-spectrum antibiotic therapy. It is known that long-term administration of the antibiotics cause the bacterium alternation and to cause IFI. Surprisingly, 11 out of 23 IFI patients were found with AML. Treatment strategies in many pediatric AML study groups have similarities, including risk-group directed treatment, the use of similar drugs (cytarabine, anthracycline, and etoposide), and blockwise therapy.[14] We used the AML99 and AML98 pilot protocols for patients with AML.[15] These protocols include etoposide, cytarabine, and mitoxantrone as induction therapy and their use has brought about an improvement in survival rate; however, the period of bone marrow suppression is long and infection can occur

TABLE 3. Risk Factors for Invasive Fungal Infection Based on Univariate Analysis

	IFI (n = 23)	No IFI (n = 311)	*P*
Sex			
Male	13	185	0.828
Female	10	126	
Age at admission			
Median	12.1 (0-18.4)	5.0 (0-29.6)	< 0.001
< 10 y	9	223	0.002
≥ 10 y	14	88	
Disease			
Malignant	21	262	0.550
Nonmalignant	2	49	
AML			
Yes	11	40	< 0.001
No	12	271	
History of SCT			
Yes	11	123	0.510
No	12	188	
Year			
-2001	5	117	0.178
2002-	18	194	
Condition of disease			
Relapse	11	50	0.001
No relapse	12	261	
Long-term administration of broad-spectrum antibiotics (> 1 wk)			
Yes	23	245	0.011
No	0	66	
Long-term administration of steroid (> 1 wk, > 1 mg/kg)			
Yes	14	166	0.523
No	9	145	

AML indicates acute myelogenous leukemia; IFI, invasive fungal infection; SCT, stem-cell transplantation.

TABLE 4. Multivariate Analysis of Risk Factors for Invasive Fungal Infection

Factor	Hazard Ratio		*P*	CI
AML	Yes	11.460	0.001	1.969-12.701
Age at admission	≥ 10 y	8.463	0.004	1.573-10.223
Relapse	Yes	6.872	0.009	1.368-8.754

AML indicates acute myelogenous leukemia; CI, confidence interval.

easily. In the 11 IFI patients with AML, IFI occurred after SCT in 4 patients, at the time of reinduction therapy in 4 patients, and during consolidation therapy in 3 patients. The relapse rate was relatively high in patients with AML, compared with those with acute lymphoblastic leukemia; therefore, many AML patients have an indication for SCT and this may be one of the reasons why IFI occurred more frequently in patients with AML. Lehrnbecher et al[16] reported that the majority of children with AML receives at least 1 episode of antifungal therapy in AML-BFM 93 study.

On the other hand, age above 10 years on admission was another risk factor for IFI in our study. Age at occurrence of AML was also relatively high and this may also explain the higher occurrence of IFI in these patients. Previous studies have suggested that age is a risk factor for IFI in children [10,11] and we have reported that age is an independent risk factor not only for IFI in AML but also for patients after SCT.[13] In the current study, older patients did not receive more intensive chemotherapy; therefore, AML is a risk factor for IFI that is independent of age, as shown by multivariate analysis. It is unclear why age is a risk factor for IFI, but this finding may reflect the importance of host colonization by environmental fungi as an important step in development of invasive disease, with younger patients having had less exposure time to fungal spores in the environment.[17] In addition, injury to the mucous membrane by chemotherapy occurs more easily in older children; as fungi invade from the mucous membrane of the intestine, this may account for higher age as a risk factor for IFI.[18]

In our patients, the mortality of IFI was 48.2%, excluding patients with relapse and IP, and was especially high in patients with a fungal lung infection, 71.4% of whom died due to IFI. This may be because the symptoms of a lung lesion, cough and low-grade fever, may also be due to other respiratory infections; and furthermore, *Aspergillus*, the most common cause of a lung lesion, is resistant to fluconazole. Many patients received treatment with multiple antifungal drugs, but the mortality of patients with IFI was very high. Therefore, early diagnosis of IFI is extremely important for a patient with prolonged fever, especially if the patient has AML and is an older child. In conclusion, our results show that AML and age are risk factors for IFI in patients with hematologic diseases and malignancies. We are trying prevention for IFI using voriconazole in patients with AML. However, cost of voriconazole is high and it is known that invasive zygomycosis increase in patients with voriconazole prophylaxis.[19] Breakthrough infection is known during use of micafungin also. However, we might have to think prophylactic usage of micafungin for patients with high risk of IFI. The mortality of patients complicated with IFI is very high, making prophylactic administration of antifungal drugs and early diagnosis and treatment very important.

REFERENCES

1. Frickhofen N, Kaltwasser JP, Schrezenmeier H, et al. Treatment of aplastic anemia with antithymocyte globulin and methylprednisolone with or without cyclosporine. *N Eng J Med.* 1991;324: 1297–1304.
2. Kojima S, Hibi S, Kosaka Y, et al. Immunosuppressive therapy using antithymocyte globulin, cyclosporine, and danazol with or without human granulocyte colony-stimulating factor in children with acquired aplastic anemia. *Blood.* 2000;96:2049–2054.
3. Chandrasekar PH, Weinmann A, Shearer C. Autopsy identified infections among bone marrow transplant recipients: a clinicopathologic study of 56 patients. *Bone Marrow Transplant.* 1995;16: 676–681.
4. Donnelly JP. Symptoms and diagnosis of nosocomial fungal infections–state-of-the-art. *Eur J Med Res.* 2003;7:192–199.
5. Erjavec Z, Verweij PE. Recent progress in the diagnosis of fungal infections in the immunocompromised host. *Drug Resist Update.* 2002;5:3–10.
6. Zaoutis TE, Benjamin DK, Steinbach WJ. Antifungal treatment in pediatric patients. *Drug Resist Updat.* 2005;8:235–245.
7. Steinbach WJ, Walsh TJ. Mycoses in pediatric patients. *Infect Dis Clin North Am.* 2006;20:663–678.
8. Hovi L, Saarinen-Pihkala UM, Vettenranta K, et al. Invasive fungal infections in pediatric bone marrow transplant recipients: single center experience of 10 years. *Bone Marrow Transplant.* 2000;26: 999–1004.
9. Benjamin DK Jr, Miller WC, Bayliff S, et al. Infections diagnosed in the first year after pediatric stem cell transplantation. *Pediatr Infect Dis J.* 2002;21:227–234.
10. Dvorak CC, Steinbach WJ, Brown JM, et al. Risks and outcomes of invasive fungal infections in pediatric patients undergoing allogeneic hematopoietic cell transplantation. *Bone Marrow Transplant.* 2005; 36:621–629.
11. Rosen GP, Nielsen K, Glenn S, et al. Invasive fungal infections in pediatric oncology patients: 11-year experience at a single institution. *J Pediatr Hematol Oncol.* 2005;27:135–140.
12. Ascioglu S, Rex JH, de Pauw B, et al; Invasive Fungal Infections Cooperative Group of the European Organization for Research and Treatment of Cancer; Mycoses Study Group of the National Institute of Allergy and Infectious Diseases. Defining opportunistic invasive fungal infections in immunocompromised patients with cancer and hematopoietic stem cell transplants: an international consensus. *Clin Infect Dis.* 2002;34:7–14.
13. Kobayashi R, Kaneda M, Sato T, et al. Evaluation of risk factors for invasive fungal infection after allogeneic stem cell transplantation in pediatric patients. *J Pediatr Hematol Oncol.* 2007;29: 786–791.
14. Kaspers GJ, Creutzig U. Pediatric acute myeloid leukemia: international progress and future directions. *Leukemia.* 2005;19: 2025–2029.
15. Kobayashi R, Tawa A, Hanada R, et al. Extramedullary infiltration at diagnosis and prognosis in children with acute myelogenous leukemia. *Pediatr Blood Cancer.* 2007;48:393–398.
16. Lehrnbecher T, Kaiser J, Varwig D, et al. Antifungal usage in children undergoing intensive treatment for acute myeloid leukemia: analysis of the multicenter clinical trial AML-BFM 93. *Eur J Clin Microbiol Infect Dis.* 2007;26:735–738.
17. Dini G, Castagnola E, Comoli P, et al. Infections after stem cell transplantation in children: state of the art and recommendations. *Bone Marrow Transplant.* 2001;28(suppl 1):S18–S21.
18. Peters M, Weiner J, Whelan G. Fungal infection associated with gastroduodenal ulceration: endoscopic and pathologic appearances. *Gastroenterology.* 1980;78:350–354.
19. Siwek GT, Dodgson KJ, de Magalhaes-Silverman M, et al. Invasive zygomycosis in hematopoietic stem cell transplant recipients receiving voriconazole prophylaxis. *Clin Infect Dis.* 2004;39: 584–587.

A 5-Year-Old Boy With Unicentric Castleman Disease Affecting the Mesentery

Utility of Serum IL-6 Level and ^{18}F-FDG PET for Diagnosis

Nariaki Toita, MD, PhD, Nobuaki Kawamura, MD, PhD,* Norikazu Hatano, MD,* Syun-ichiro Takezaki, MD,* Yuka Ohkura, MD,* Masafumi Yamada, MD, PhD,* Motohiko Okano, MD, PhD,* Tadao Okada, MD, PhD,† Fumiaki Sasaki, MD, PhD,† Kanako C. Kubota, MD, PhD,‡ Tomoo Itoh, MD, PhD,§ and Tadashi Ariga, MD, PhD**

Summary: Castleman disease (CD) is a rare lymphoproliferative disorder of unknown etiology. It is quite difficult to diagnose CD without typical localized signs or symptoms. We present a 5-year-old boy with unicentric plasma cell CD in the mesentery, which was too small to be detected by any conventional imaging. ^{18}F-fluorodeoxyglucose positron emission tomography image and a serum cytokine profile prompted us to perform a curative surgical excision, confirming his diagnosis. Our case also supported an important role of interleukin-6 in the pathophysiology of plasma cell CD.

Key Words: Castleman disease, lymphoproliferative disorder, ^{18}F-FDG PET, mesentery, interleukin-6

(*J Pediatr Hematol Oncol* 2009;31:693–695)

Castleman disease (CD) is a rare disorder of lymph node hyperplasia with an unknown etiology.[1] CD is divided into 2 clinical subtypes: unicentric and multicentric varieties. Unicentric disease manifests as a solitary mass that most often affects younger patients. Multicentric disease has systemic manifestations and is relatively rare in children. CD can be histologically classified into 2 major types: the hyaline-vascular type, which accounts for more than 90% of the cases and is usually asymptomatic and the less common plasma-cell type, which is almost always associated with systemic manifestations such as fever, weight loss, anemia, elevated sedimentation rate, and polyclonal hypergammaglobulinemia.[2] Most cases with hyaline-vascular CD are found by chance, whereas plasma cell CD may occasionally be the cause of fever from an unknown origin. Computed tomography (CT) and ultrasonography are useful methods to find CD foci. ^{67}Gallium (Ga) scintigraphy may be a more sensitive tool for the detection of CD especially in a case with no localized signs,[3] but not all cases always show abnormal uptake.[4,5] We present here a 5-year-old boy with unicentric plasma cell CD, whose disease focus could only be detected by ^{18}F-fluorodeoxyglucose positron emission tomography (^{18}F-FDG PET) and not by ^{67}Ga scintigraphy.

Received for publication December 11, 2008; accepted May 4, 2009.
From the Departments of *Pediatrics; †Pediatric Surgery, Graduate School of Medicine; ‡Department of Surgical Pathology, Hokkaido University Hospital, Sapporo; and §Division of Diagnostic Pathology, Kobe University Graduate School of Medicine, Hyogo, Japan.
This study was supported by Grant-in-Aid for Scientific Research from the Japanese Ministry of Health, Labor and Welfare (2542002917, 15COE011-02, and H19-Child-General-003).
Reprints: Nobuaki Kawamura, MD, PhD, Department of Pediatrics, Graduate School of Medicine, Hokkaido University Hospital, North –15, West 7, Kita-ku, Sapporo, Japan (e-mail: nobu-ka@med.hokudai.ac.jp).

CASE REPORT

A 5-year-old Japanese boy was admitted to a general hospital because of persistent high fever. He had no other significant symptoms or signs. Laboratory examination of his peripheral blood showed mild anemia and elevated C-reactive protein (CRP). All images, including whole body CT scan, abdominal ultrasonography, and ^{67}Ga scintigraphy failed to reveal any abnormal findings. Despite extensive investigations, the origin of his fever was still unknown. Owing to his fever and persistent elevated serum CRP over a long period, steroid therapy was started for possible systemic juvenile idiopathic arthritis. However, all the medications including methotrexate, cyclosporine A, and cyclophosphamide failed to normalize his abnormal laboratory findings. Then he was referred to Hokkaido University Hospital for further diagnosis.

Physical examination showed no particular signs such as a rash, lymphadenopathy, hepatosplenomegaly, or arthritis. Laboratory examination of his peripheral blood showed mild anemia (hemoglobin 11.0 g/dL and mean cell volume 70.1 fl), increased erythrocyte sedimentation rate (57 mm/h), and elevated CRP (7.92 mg/dL). The white blood cell count was 11.9×10^9/L and the platelet count was 332×10^9/L. The serum level of IgG, IgA, and IgM were 654, 94, and 113 mg/dL, respectively. The serum cytokine levels were as follows: interleukin (IL)-6 24.2 pg/mL (normal < 4.0), IL-1β < 10 pg/mL, interferon-γ < 0.1 IU/mL, and tumor necrosis factor-α < 5.0 pg/mL. As steroid treatment was gradually tapered, CRP became elevated (Fig. 1). CT scan and ^{67}Ga scintigraphy failed to show any abnormal findings over his whole body. We therefore tried ^{18}F-FDG PET to detect possible concealed inflammatory lesions such as vasculitis or CD. ^{18}F-FDG PET clearly illustrated a solitary, isolated lesion in the middle of his abdomen (Fig. 2A). Therefore, we decided to remove this single lesion surgically, expecting to get both definite diagnosis and recovery from his illness. The exploratory laparoscopy revealed a round and well-defined solid mass located in the root of the mesentery without any other enlarged lymph nodes (Fig. 2B). The mass was completely removed and measured 2.7 × 2.0 × 2.0 cms in size. Histopathologic examination of the encapsulated mass confirmed a diagnosis of plasma cell CD, characterized by the germinal centers with the sheets of plasma cell and the absence of any vascular proliferation (Figs. 3A, B). The high expression of human IL-6 gene in the excised mass was demonstrated by reverse transcription-polymerase chain reaction (RT-PCR) (Fig. 3C). Other proinflammatory cytokine genes were not expressed in the same specimens. Human herpes virus (HHV)-8 DNA in the mass

CLINICAL AND VACCINE IMMUNOLOGY, Jan. 2010, p. 190–193 Vol. 17, No. 1
1556-6811/10/$12.00 doi:10.1128/CVI.00355-09

Antibodies against Structural and Nonstructural Proteins of Human Bocavirus in Human Sera[▽]

Reza Shirkoohi,[1]† Rika Endo,[1,2]† Nobuhisa Ishiguro,[1]* Shinobu Teramoto,[1] Hideaki Kikuta,[3] and Tadashi Ariga[1]

Department of Pediatrics[1] and Department of Microbiology,[2] Hokkaido University Graduate School of Medicine, and Pediatric Clinic, Touei Hospital,[3] Sapporo, Japan

Received 4 September 2009/Returned for modification 20 October 2009/Accepted 18 November 2009

Immunofluorescence assays (IFAs) for detection of human bocavirus (HBoV) proteins (VP1, VP2, NP-1, and NS1) were developed. The VP1 IFA was the most sensitive for detection of IgG antibody and suitable for screening. IgG antibodies in convalescent-phase sera from HBoV-positive patients were detected by VP1 and VP2 IFAs. Sensitivities of NP-1 and NS1 IFAs were low.

Human bocavirus (HBoV), belonging to the family *Parvoviridae*, subfamily *Parvovirinae*, and genus *Bocavirus*, was cloned by molecular screening of pooled human respiratory tract samples in 2005 (2). Until the identification of HBoV, human parvovirus B19 (subfamily *Parvovirinae*, genus *Erythrovirus*) had been the only known human pathogen in the family *Parvoviridae* (42). HBoV has been detected in patients with respiratory tract infections in many countries by PCR or real-time PCR, the rate of HBoV detection ranging from 1.5 to 19% (1, 3–5, 8, 9, 13, 14, 24, 26–28, 30, 31, 33, 35–39, 41). However, the causative role of HBoV in respiratory tract infection remains unclear. In fact, HBoV is codetected with other respiratory viruses in many cases of lower respiratory tract infection (1, 3, 8, 9, 13, 14, 20, 30, 34, 39, 41).

Real-time PCR for HBoV has been used to analyze the pathophysiology of HBoV infections. High loads of HBoV in nasopharyngeal samples, mainly in the absence of other viral agents, have been found in some studies, suggesting a causative role in acute respiratory tract infections (1, 17). Another study showed that the load of HBoV in nasopharyngeal samples from patients with bronchiolitis was significantly higher than that in patients with the diagnosis of febrile seizures (34).

Seroepidemiological study is also an important tool for diagnosis of and research on HBoV infection. Antibodies against HBoV in serum are raised after HBoV infection, suggesting that HBoV infection evokes a systemic immune response (11, 18, 19, 23). Recently, we developed an immunofluorescence assay (IFA) to measure titers of specific antibodies against HBoV VP1, which is one of the structural proteins of HBoV (11). HBoV encodes two structural proteins (VP1 and VP2) and two nonstructural proteins (NP-1 and NS1) (2). The recombinant structural proteins (VP1 and VP2) of B19 have been used for the detection of IgG and IgM antibodies against B19 (6, 22). More recently, the nonstructural protein (NS1) of B19 was shown to play a significant role in serodiagnosis of acute infection, thereby supplementing the role played by B19 structural proteins as diagnostic antigens (10, 12, 15). The purpose of this study was to compare the efficiencies of IFAs using individual proteins of HBoV.

A baculovirus expression kit (Bac-to-Bac system) was used to prepare histidine (His)-tagged VP1, VP2, NP-1, and NS1 proteins for expression in a baculovirus-insect cell system in accordance with the instructions of the manufacturer (Invitrogen, Carlsbad, CA). The genomic DNA corresponding to VP1, VP2, NP-1, and NS1 proteins of HBoV from strain JPBS05-52 (GenBank accession numbers EF035488, EU984096, and EU984097) was amplified by PCR with the following primers: HBoV VP1 start (5′-ATC GTC TCG CAT GAG TAA AGA AAG TGG CAA-3′), HBoV VP2 start (5′-ATC GTC TCG CAT GTC TGA CA CTG ACA TTC A-3′), HBoV VP1 and VP2 end (5′-GCC TCG AGT TAC AAT GGG TGC ACA CGG C-3′), HBoV NP-1 start (5′-ATC GTC TCG CAT GAG CTC AGG GAA TAT GAA-3′), HBoV NP-1 end (5′-GCC TCG AGT TAA TTG GAG GCA TCT GCT T-3′), HBoV NS1 start (5′-ATC CAT GGC TTT CAA TCC TCC T-3′), and HBoV NS1 end (5′-CGC TCG AGT TAC TTA CTT GGT G-3′) (the restriction sites in the primers used for cloning are underlined). The following procedures for making baculoviruses were described previously (11). *Trichoplusia ni* (Tn5) cells in T25 flasks were infected with recombinant baculoviruses expressing His-tagged VP1, VP2, NP-1, and NS1 proteins of HBoV and with mock baculovirus at a multiplicity of infection of 10 virus particles per cell and were resuspended in 250 μl of phosphate-buffered saline (PBS). The procedures for Western blot analysis were described previously (11). The results of Western blot analysis are shown in Fig. 1A. The predicted molecular sizes of His-VP1, His-VP2, His-NP-1, and His-NS1 fusion proteins of HBoV were 78.1, 63.4, 29.0, and 75.0 kDa, respectively, which were consistent with the molecular sizes of these proteins determined by Western blotting using anti-six-histidine tag monoclonal antibody.

IFAs using Tn5 cells infected with recombinant baculoviruses expressing VP1, VP2, NP-1, and NS1 proteins of HBoV were developed as described previously (11, 16). A total of 205 serum samples were randomly obtained from outpatients or

* Corresponding author. Mailing address: Department of Pediatrics, Hokkaido University Graduate School of Medicine, N-15, W-7, Kita-ku, Sapporo 060-8638, Japan. Phone: 81-11-706-5954. Fax: 81-11-706-7898. E-mail: nishigur@med.hokudai.ac.jp.

† R.S. and R.E. contributed equally to the research described in this paper.

▽ Published ahead of print on 2 December 2009.

ARTICLE IN PRESS

YBCMD-01383; No. of pages: 5; 4C: 3

Blood Cells, Molecules, and Diseases xxx (2010) xxx–xxx

Contents lists available at ScienceDirect

Blood Cells, Molecules, and Diseases

journal homepage: www.elsevier.com/locate/ybcmd

X-linked agammaglobulinemia in a 10-year-old boy with a novel non-invariant splice-site mutation in *Btk* gene

Kota Maekawa [a], Masafumi Yamada [a,*], Yuka Okura [a], Yasumasa Sato [b], Yutaka Yamada [b], Nobuaki Kawamura [a], Tadashi Ariga [a]

[a] *Department of Pediatrics, Hokkaido University Graduate School of Medicine, Sapporo, 060-8638, Japan*
[b] *Department of Pediatrics, Hakodate Central General Hospital, Hakodate, 040-8585, Japan*

ARTICLE INFO

Article history:
Submitted 2 September 2009
Revised 16 December 2009
Available online xxxx

(Communicated by R. I. Handin, M.D.,
05 January 2010)

Keywords:
X-linked agammaglobulinemia (XLA)
Bruton's tyrosine kinase (Btk)
Non-invariant splice-site mutation
Significant levels of serum immunoglobulins

ABSTRACT

X-linked agammaglobulinemia (XLA) is a primary immunodeficiency disease caused by mutations in the gene coding for Bruton's tyrosine kinase (Btk). Most XLA patients have severely reduced or absent peripheral blood B cells and serum immunoglobulins, since the expression or function of Btk, critical for the maturation of B cell lineages at pro-B and pre-B cell stages, is deficient. Early and accurate diagnosis of XLA is important, since the affected patients suffer from severe and recurrent infections unless they receive intravenous immunoglobulin (IVIG) replacement therapy. However, the diagnosis of XLA is not always easy because some patients have detectable (~2%) B cells in the peripheral blood and have significant levels of serum immunoglobulins. In this study, we report on a patient who was diagnosed with XLA at the age of 10 years. The diagnosis was delayed due to near-normal levels of serum immunoglobulins, although he presented with severe and recurrent bacterial infections since the age of 1 year. He was demonstrated to have a novel non-invariant splice-site mutation in intron 10 (IVS10 −11C→A) of the *Btk* gene, which was not detected by the standard PCR-based mutation analysis. This mutation resulted in no detectable Btk expression. This case suggests that patients suffering from severe or recurrent bacterial infection should be suspected to have XLA even though they may have significant levels of serum immunoglobulins. Furthermore, significant levels of serum immunoglobulins in XLA patients do not necessarily mean less severe phenotype.

Introduction

X-linked agammaglobulinemia (XLA) is a primary immunodeficiency disease first described by Bruton in 1952 [1]. It is characterized by marked reduction in serum levels of all immunoglobulin isotypes, defective B cell development at pro-B and pre-B cell stages [2,3] and severely decreased numbers of circulating B cells. Affected males have susceptibility to severe bacterial infections unless they receive appropriate therapy, including intravenous immunoglobulin (IVIG) replacement therapy. Since the gene responsible for XLA was identified as coding for a cytoplasmic tyrosine kinase named Bruton's tyrosine kinase (Btk), various mutations have been reported [4–7]. However, the direct detection of *Btk* mutations by sequence analysis is time-consuming as a diagnostic procedure. Furthermore, some XLA patients have detectable (~2%) B cells in the peripheral blood and/or show significant levels of serum IgG (~800 mg/dl), which makes the diagnosis of XLA difficult. Flow cytometric analysis of Btk expression (FCM-Btk) is one of the simple and useful methods for the diagnosis of XLA [7]. In this study, we report on a patient who was given the diagnosis of XLA at the relatively advanced age of 10 years. The delay in diagnosis was apparently due to the presence of near-normal levels of serum immunoglobulins, although he presented with severe and recurrent infections since the age of 1 year. He was demonstrated to have a novel non-invariant splice-site mutation in intron 10 (IVS10 −11C→A) of the *Btk* gene, which was not detected by the standard PCR-based mutation analysis. Although splice-site mutations sometimes result in partial ("leaky") expression of Btk, this mutation resulted in no detectable Btk expression.

Materials and methods

Subjects

Samples of three unrelated XLA patients confirmed by *Btk* mutations were used as Btk-deficient controls. The patient, W.I., had suffered from recurrent episodes of acute otitis media, sinusitis, lymphadenitis with abscess, and colitis since the age of 1 year. He also had repetitive episodes of high fever with marked leukocytosis and elevation of CRP (~20 mg/dl). Every time, he was suspected to have bacterial septicemia or meningitis and was treated with intravenous antibiotics effectively, although focus of infection was not identified. He had no family history of severe infections or immunodeficiency. His recent

* Corresponding author. Hokkaido University Graduate School of Medicine, Department of Pediatrics, North 15 West 7, Kita-ku Sapporo, 060-8638, Japan.
E-mail address: yamadam@med.hokudai.ac.jp (M. Yamada).

1079-9796/$ – see front matter © 2010 Elsevier Inc. All rights reserved.
doi:10.1016/j.bcmd.2010.01.004

Table 1
Primers used for *Btk* RT-PCR and intron 10 PCR studies.

Primers for *Btk* RT-PCR	Sequence	Tm (°C)	Corresponding exon (s)
Forward			
Btk1F	5′- gac tgt cct tcc tct ctg ga -3′	54	1
Btk2F	5′- ctt caa gaa gcg cct gtt tct -3′	52	2
Btk3F	5′- cat tga aag att ccc tta tcc c -3′	51	4
Btk4F	5′- atg ggc tgc caa att ttg gag -3′	52	6
Btk5F	5′- tga tta cat gcc aat gaa tgc -3′	49	8
Btk6F	5′- gct cat taa cta cca tca gca c -3′	53	12
Btk6F-2	5′- cat tga aga agc caa agt c -3′	47	14
Btk7F	5′- ccg gaa gtc ctg atg tat ag -3′	52	17
BtkNoF	5′- agc aag agg gga aag aag gag	54	10–11
Reverse			
Btk1R	5′- acc ctt ctt act gcc tct tc -3′	52	3
Btk2R	5′- aat cca ccg ctt cct tag ttc -3′	52	5
Btk3R	5′- tca ggc gtt ggg gga aga ggc -3′	60	7
Btk4R	5′- cta gga atg tag cct tcc tgc -3′	54	9
Btk5R	5′- gca gtg gaa ggt gca ttc ttg -3′	54	13
Btk6R	5′- ggc cga aat cag ata ctt t -3′	47	16
Btk7R	5′- agc ttg gga ttt cct ctg aga -3′	59	19
Primers for *Btk* intron 10 PCR	Sequence	Tm (°C)	Corresponding exon/intron
Intron 10F1	5′- gag caa ctg cta aag caa gag -3′	52	exon 10
Intron 10F2	5′- gtc tcg aac tcc tga cct cag -3′	56	intron 10
Intron 10R1	5′- ctg tgg att tag caa aca cag -3′	50	exon 11

serum immunoglobulin levels were: IgG 400–800 mg/dl (normal range: 608–1572 mg/dl), IgA of 4–5 mg/dl (normal range: 33–236 mg/dl), and IgM of 64–102 mg/dl (normal range: 52–242 mg/dl). However, he failed to develop specific IgG antibodies against all the immunizations he received (rubella, measles and mumps), and had no antibodies against Epstein–Barr virus (EBV) and Cytomegalovirus (CMV). He had not received further laboratory studies because of near-normal levels of immunoglobulins. The proportion of his peripheral blood lymphocytes that were CD19+ cells (B cells) at the age of 8 years and 10 years was significantly reduced to be 0.6% and 0.2%, respectively. He was referred to our hospital for further evaluation of B cell deficiency at the age of 10 years.

Flow cytometric analysis of intracellular Btk expression (FCM-Btk) in monocytes

We performed FCM-Btk, originally established by Futatani et al. [7], basically following the WASP detection protocol established for the diagnosis of Wiskott–Aldrich syndrome [8]. Briefly, heparinized blood samples were collected from a patient and a normal individual under the same conditions. Peripheral blood mononuclear cells (PBMC) isolated by standard Ficoll-Hypaque gradient centrifugation methods were washed with phosphate-buffered saline (PBS) containing 1% fetal bovine serum. Cell pellets were resuspended with 100 μl of Cytofix/Cytoperm solution (BD Biosciences, San Diego, CA) and incubated at 4 °C for 20 min. After three washes with Perm/Wash solution, they were incubated with 1 μg/ml of anti-Btk antibody (48-2H) [9] or MOPC21 mouse IgG1 control (Sigma, Saint Louis, MO) at 4 °C for 30 min and washed three times. They were then reacted with 1 μg/ml of fluorescein isothiocyanate (FITC)-conjugated goat anti-mouse IgG1 (Southern Biotechnology Associates, Birmingham, AL) at 4 °C for 30 min and washed three times. Samples were then analyzed on a FACSCalibur (BD Biosciences). A total of 20,000 events of monocytes, which were gated based on forward and side scatter, were analyzed.

PCR, RT-PCR, and Btk sequence analysis

SepaGene (Sanko Junyaku, Tokyo, Japan) and TRIzol Reagent (Invitrogen, Carlsbad, CA) were used for the isolation of DNA and total RNA from PBMC, respectively. *Btk* exons, adjacent intronic regions, and a putative promoter region were amplified by PCR with primers

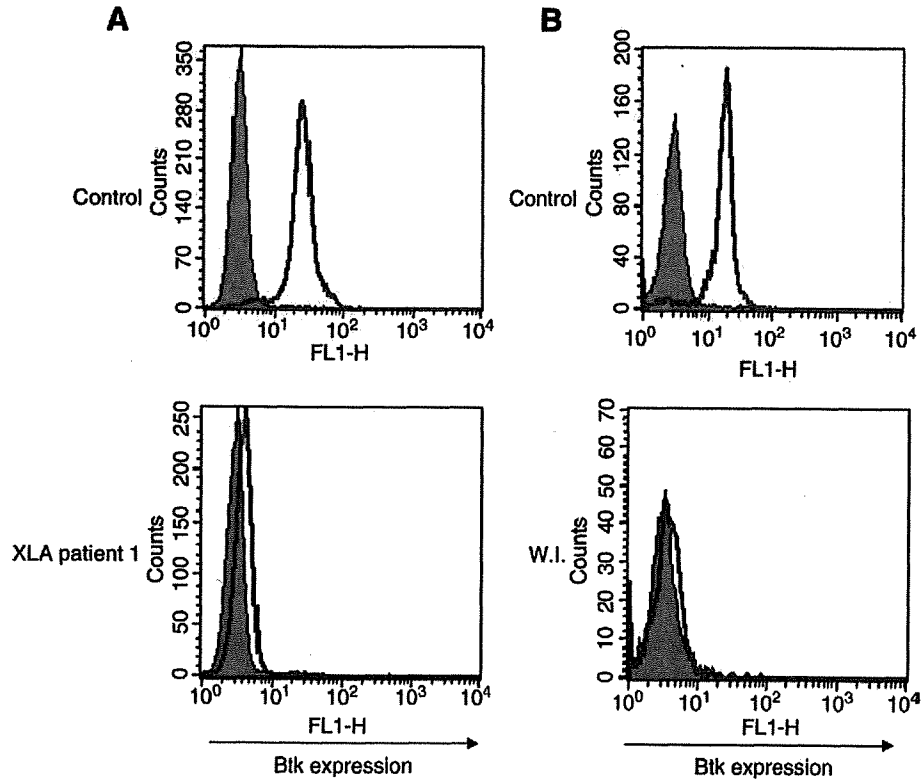

Fig. 1. Flow cytometric analysis of intracellular Btk expression (FCM-Btk) in monocytes ▩: isotypic control, ■: anti-Btk antibody (48-2H). A: FCM-Btk result of a normal control (Control) and a known XLA patient (XLA patient 1). B: FCM-Btk result of a normal control (Control) and the patient, W.I.

Please cite this article as: K. Maekawa, et al., X-linked agammaglobulinemia in a 10-year-old boy with a novel non-invariant splice-site mutation in *Btk* gene, Blood Cells Mol. Diseases (2010), doi:10.1016/j.bcmd.2010.01.004

described by Vorechovský et al. [10]. For the analysis of the whole sequence of intron 10, we performed PCR with a combination of Intron 10F1 and Intron 10R1 primers and a combination of Intron 10F2 and Intron 10R1 primers (Table 1). Intron 11 full sequences were studied with a combination of exon 10 forward and exon 11 reverse primers described by Vorechovský et al. [10]. RT-PCR was performed using the primers described in Table 1 after the preparation of complementary DNA (cDNA) from total RNA using 1st Strand cDNA Kit (GE Healthcare Buckinghamshire, UK). The primer BtkNoF was designed to match the exon 10–exon 11 junction to specifically amplify only wild-type transcripts (Table 1). PCR and RT-PCR products isolated by Gel-purification kit (Invitrogen) were then directly sequenced using BigDye Terminator Cycle Sequencing Kits v1.1 (Applied Biosystems, Carlsbad, CA). "Splice Site Prediction by Neural Network" (www.fruitfly.org/seq_tools/splice.html) was used for the prediction of splice sites.

Western blot analysis of Btk expression

PBMC pellets from normal controls and XLA patients were resuspended in cytoplasmic extract buffer containing 0.5% Nonidet P-40, 250 mM NaCl, 10 mM HEPES pH 7.9, 0.1 mM EDTA, 1 mM Na_3VO_4, 1 mM NaF, pH 8.0 with the addition of the recommended volume of dissolved protease inhibitor cocktail tablets (Roche, Basel, Switzerland). After incubation on ice for 15 min, the supernatant after centrifugation at maximum speed for 5 min at 4 °C was saved as cytoplasmic extract. Protein concentration was measured by Protein Assay (Bio-Rad, Hercules, CA). Thirty micrograms of cytoplasmic extract after addition of SDS sample buffer was separated by 8% polyacrylamide gels and transferred to Hybond-P PVDF membranes (GE Healthcare). Two anti-Btk monoclonal antibodies were used: 48-2H [9] and 8E5.A10.E5 [11] corresponding to SH3 and PH domains of Btk, respectively. Anti-actin antibody (AC40) was purchased from Sigma. All the primary antibodies were used at the final concentration of 1 μg/ml. Horseradish peroxidase (HRP)-conjugated anti-mouse IgG secondary antibodies (GE Healthcare) were used at 1:2000 dilution. The blots were then visualized by ECL plus (GE Healthcare).

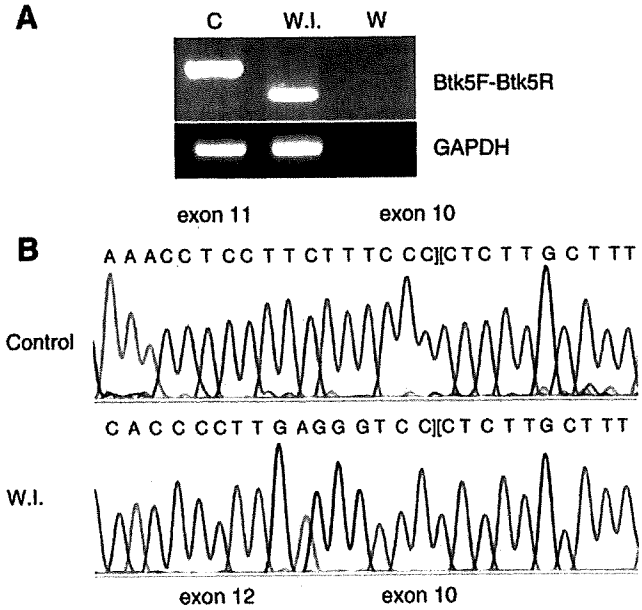

Fig. 2. RT-PCR analysis of *Btk* followed by sequence analysis. A: Samples of a control (C), the patient, W.I., and water (W) after RT-PCR with Btk5F and Btk5R primers were separated on agarose gel. The housekeeping gene GAPDH was used as a positive control for the presence of mRNA in the samples. B: Direct sequence analysis of RT-PCR products from a control (Control) and W.I. Reverse sequence was shown.

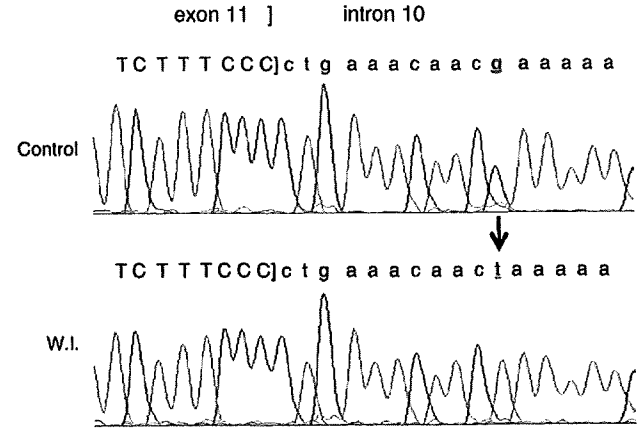

Fig. 3. Direct sequence analysis of samples from a normal control (Control) and W.I. after PCR with Intron 10F2 and Intron 10R1 primers. Reverse sequence was shown.

Results

First of all, we performed flow cytometric analysis of intracellular Btk protein expression (FCM-Btk) in monocytes from the possible XLA patient, W.I., who had severe and recurrent infections in spite of consistently showing near-normal levels of serum IgG. Patient, W.I, as well as 3 XLA patients confirmed by detection of *Btk* mutations was demonstrated to have deficient Btk expression, indicating he has XLA (Fig. 1 and data not shown). We then proceeded to a molecular study of *Btk* gene using the standard PCR-based mutation analysis with primers as described by Vorechovský et al. [10]. Unexpectedly, no mutations were detected in direct sequence analysis of all the exons, exon–intron boundaries and a putative promoter region of this gene. However, the study of the Btk mRNA expression by RT-PCR and the subsequent direct sequence analysis of these products demonstrated that he had a shorter RT-PCR product with Btk5F (a forward primer in exon 8) and Btk5R (a reverse primer in exon 13), which resulted from skipping of exon 11 (Fig. 2). RT-PCR products amplified from other parts of the mRNA were normal in size and sequences. To identify the mechanism of exon 11 skipping, we performed direct sequence analysis of the whole intron 10 and intron 11 as described in Materials and methods. The results demonstrated that he had wild-type sequences except a base change in intron 10, 11 bases upstream of exon 11 (Fig. 3). This base change was found to be included in the middle of the forward primer used for sequence analysis of the intron 10–exon 11 boundary [10]. His mother showed c+a signals at this site (data not shown), indicating that his mother is heterozygous for this base change. "Splice Site Prediction by Neural Network" analysis of the sequence of the intron 10–exon 11 junction gave a significantly lower score for the sequence with the patient's mutation (0.80), compared with that of wild-type sequence (0.93) (Fig. 4). These

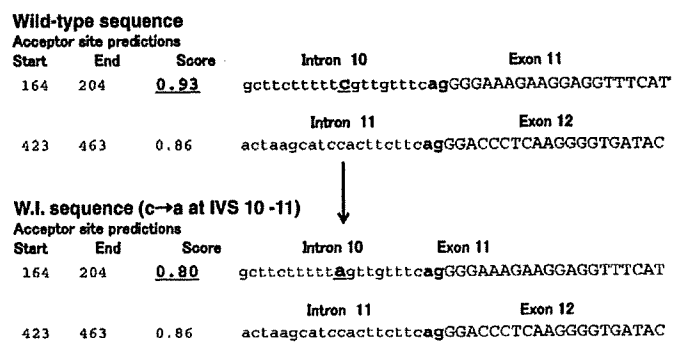

Fig. 4. The results of predicted splice sites with "Splice Site Prediction by Neural Network" (http://www.fruitfly.org/seq_tools/splice.html) were shown.

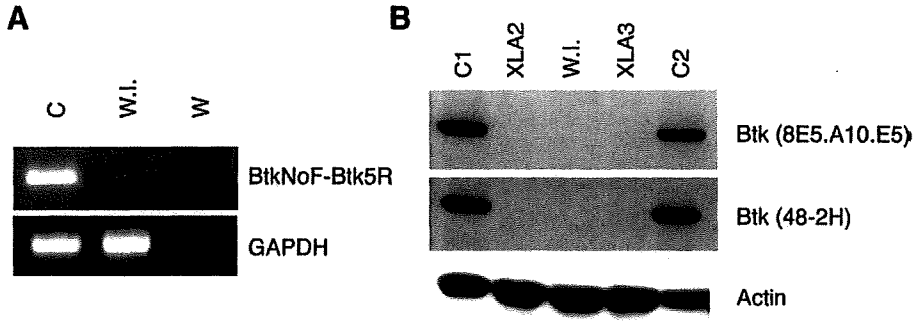

Fig. 5. Study of possible leaky expression of normal *Btk* transcripts and Btk expression. A: Control (C), W.I., and water (W) samples after RT-PCR with BtkNoF and Btk5R primers were separated on agarose gel. The housekeeping gene GAPDH was used as a positive control for the presence of mRNA in the samples. B: Western blot analysis of Btk expression in PBMC from two controls (C1 and C2), two XLA patients (XLA2 and XLA3), and the patient, W.I. Actin expression was used as a loading control.

results suggest that the base change of IVS10 −11C→A is a novel splice-site mutation leading to skipping of exon 11, which was predicted to cause frameshift and premature termination of protein translation, 23 codons downstream from the end of exon 10. Since the mutation is not within the invariant GT or AG splice site (the first two or the last two base pairs of an intron), it was possible that low levels of normal Btk message could be transcribed due to a leaky splicing defect. To study this possibility, we performed RT-PCR with a primer corresponding to the exon 10–exon 11 junction (BtkNoF) and Btk5R to specifically amplify only wild-type transcripts. The result, however, demonstrated that W.I. had no wild-type transcripts of *Btk* gene (Fig. 5A). Consistent with this result, Western blot analysis of PBMC also demonstrated that expression of normal Btk protein was not detectable with the use of two monoclonal anti-Btk antibodies: 8E5.A10.E5 and 48-2H (Fig. 5B, Materials and methods). Since his mutation was predicted to affect the mRNA sequence downstream of exon 10, these two antibodies, 8E5.A10.E5 (corresponding to PH domain, exon 2–5) and 48-2H (corresponding to SH3 domain, exon 8–9) should detect the truncated Btk protein if it exists. However, truncated Btk expression was undetectable in his PBMC with these two antibodies (data not shown).

Discussion

In this study, we report on a patient, W.I., who was diagnosed with XLA at the age of 10 years. In spite of normal or near-normal levels of serum IgG, he presented severe and recurrent infections since the age of 1 year. He was demonstrated to have deficient Btk expression in monocytes which was caused by a novel non-invariant splice-site mutation in intron 10 (IVS10 −11C→A) of the *Btk* gene. At first, sequence analysis of the *Btk* gene using primers previously reported [10] demonstrated no mutations in all the exons, exon–intron boundaries and a putative promoter region of *Btk* gene. Based on deficient Btk expression, we considered the possibilities that he had a splice-site mutation located outside of the sequences studied or a mutation in an unknown region regulating Btk expression. RT-PCR studies revealed a skipping of exon 11 (Fig. 2), indicating a splice-site mutation in intron 10 or 11. Subsequent sequence analysis of the whole intron 10 and 11 demonstrated that he has a base change in intron 10, 11 bases upstream of exon 11 (Fig. 3), which is a non-invariant site for splice mutation. This result explains why we could not detect his mutation by the original PCR-based mutation analysis, because the mutation was in the middle of the forward primer used for sequence analysis of the intron 10–exon 11 boundary, not because it was located outside of the sequences studied. These results suggest that a combination studies at the DNA, RNA and protein levels are important to avoid overlooking a mutation of this gene that is responsible for XLA. Although no strong genotype–phenotype correlation has been established in XLA patients [12–15], some mutations in *Btk*, particularly mutations that allow Btk protein expression are likely to be associated with less severe phenotype. As for splicing defects, a few patients with mild disease were shown to have some Btk expression due to leaky splicing [16–18]. In contrast to these patients, the patient, W.I., who presented severe phenotype, was demonstrated to have absent expression of wild-type Btk both at mRNA and protein levels (Figs. 1B and 5B). He also had no truncated Btk protein expression due to skipping of exon 11. Therefore, this study indicated that the splice-site mutation of IVS10 −11C→A could be one of the mutations causing the severe, typical XLA phenotype. Some XLA patients have been shown to have significant levels of serum immunoglobulins, similar to the present case with near-normal IgG and normal IgM. This might be explained by the presence of small numbers of "leaky" mature B cells possessing the ability to proliferate, undergo class switching, and differentiate into antibody-producing cells, through unknown mechanisms independent of Btk function, as demonstrated by Nonoyama et al. [19]. It is not clear whether there is special significance to the low IgA level observed in the present case. Considering that serum IgA level is more likely to be low or undetectable even in XLA patients with normal or near-normal level of serum IgG [9,16,17,19,21], IgA production might be more dependent on Btk function, although other genetic or undefined factors might also modify it. XLA cases with significant levels of serum immunoglobulins and older age at diagnosis were generally considered as less severe phenotype [20,21]. However, at least in the present case, older age at diagnosis was associated with significant immunoglobulin concentration, but not with less severe phenotype. This case suggests that significant levels of serum immunoglobulins could be one of the factors associated with older age at diagnosis regardless of the severity of clinical phenotypes. Thus, significant levels of serum immunoglobulins in XLA patients do not necessarily mean less severe phenotype. More detailed criteria for classifying severe and less severe phenotype might be necessary to discuss genotype–phenotype correlations.

Acknowledgments

We thank Drs. Tsukada S and Kishimoto T for providing us with an anti-Btk antibody, 48-2 H, and Drs. Stewart DM and Nelson DL for providing us with an anti-Btk antibody, 8E5.A10.E5. We also thank Dr. Stewart DM for reviewing the manuscript. This work was supported in part by a grant for Research on Intractable Diseases from the Japanese Ministry of Health, Labor and Welfare.

References

[1] O.C. Bruton, Agammaglobulinemia, Pediatrics 9 (1952) 722–728.
[2] M.E. Conley, J. Rohrer, L. Rapalus, et al., Defects in early B-cell development: comparing the consequences of abnormalities in pre-BCR signaling in the human and the mouse, Immunol. Rev. 178 (2000) 75–90.
[3] J.G. Noordzij, S. de Bruin-Versteeg, W.M. Comans-Bitter, et al., Composition of precursor B-cell compartment in bone marrow from patients with X-linked

agammaglobulinemia compared with healthy children, Pediatr. Res. 51 (2002) 159–168.
[4] D. Vetrie, I. Vorechovsky, P. Sideras, et al., The gene involved in X-linked agammaglobulinemia is a member of the src family of protein-tyrosine kinases, Nature 361 (1993) 226–233.
[5] S. Tsukada, D.C. Saffran, D.J. Rawlings, et al., Deficient expression of a B cell cytoplasmic tyrosine kinase in human X-linked agammaglobulinemia, Cell 72 (1993) 279–290.
[6] J. Väliaho, C.I. Smith, M. Vihinen, BTKbase: the mutation database for X-linked agammaglobulinemia, Hum. Mutat. 27 (2006) 1209–1217.
[7] T. Futatani, T. Miyawaki, S. Tsukada, et al., Deficient expression of Bruton's tyrosine kinase in monocytes from X-linked agammaglobulinemia as evaluated by a flow cytometric analysis and its clinical application to carrier detection, Blood 91 (1998) 595–602.
[8] M. Yamada, T. Ariga, N. Kawamura, et al., Determination of carrier status for the Wiskott–Aldrich syndrome by flow cytometric analysis of Wiskott–Aldrich syndrome protein expression in peripheral blood mononuclear cells, J. Immunol. 165 (2000) 1119–1122.
[9] S. Hashimoto, S. Tsukada, M. Matsushita, et al., Identification of Bruton's tyrosine kinase (Btk) gene mutations and characterization of the derived proteins in 35 X-linked agammaglobulinemia families: a nationwide study of Btk deficiency in Japan, Blood 88 (1996) 561–573.
[10] I. Vorechovský, M. Vihinen, G. de Saint Basile, et al., DNA-based mutation analysis of Bruton's tyrosine kinase gene in patients with X-linked agammaglobulinaemia, Hum. Mol. Genet. 4 (1995) 51–58.
[11] D.M. Stewart, C.C. Kurman, D.L. Nelson, Production of monoclonal antibodies to Bruton's tyrosine kinase, Hybridoma 14 (1995) 243–246.
[12] H.B. Gaspar, L.A. Bradley, F. Katz, et al., Mutation analysis in Bruton's tyrosine kinase, the X-linked agammaglobulinemia gene, including identification of an insertional hotspot, Hum. Mol. Genet. 4 (1995) 755–757.
[13] H. Jin, A.D. Webster, M. Vihinen, et al., Identification of Btk mutations in 20 unrelated patients with X-linked agammaglobulinaemia (XLA), Hum. Mol. Genet. 4 (1995) 693–700.
[14] E. Holinski-Feder, M. Weiss, O. Brandau, et al., Mutation screening of the BTK gene in 56 families with X-linked agammaglobulinemia (XLA): 47 unique mutations without correlation to clinical course, Pediatrics 101 (1998) 276–284.
[15] S. Kobayashi, T. Iwata, M. Saito, et al., Mutations of the Btk gene in 12 unrelated families with X-linked agammaglobulinemia in Japan, Hum. Genet. 97 (1996) 424–430.
[16] H. Kaneko, N. Kawamoto, T. Asano, et al., Leaky phenotype of X-linked agammaglobulinaemia in a Japanese family, Clin. Exp. Immunol. 140 (2005) 520–523.
[17] J.G. Noordzij, S. de Bruin-Versteeg, N.G. Hartwig, et al., XLA patients with BTK splice-site mutations produce low levels of wild-type BTK transcripts, J. Clin. Immunol. 22 (2002) 306–318.
[18] D.M. Stewart, L. Tian, D.L. Nelson, A case of X-linked agammaglobulinemia diagnosed in adulthood, Clin. Immunol. 99 (2001) 94–99.
[19] S. Nonoyama, S. Tsukada, T. Yamadori, et al., Functional analysis of peripheral blood B cells in patients with X-linked agammaglobulinemia, J. Immunol. 161 (1998) 3925–3929.
[20] A. Broides, W. Yang, M.E. Conley, Genotype/phenotype correlations in X-linked agammaglobulinemia, Clin. Immunol. 118 (2006) 195–200.
[21] E. López-Granados, R. Pérez de Diego, A. Ferreira Cerdán, et al., A genotype–phenotype correlation study in a group of 54 patients with X-linked agammaglobulinemia, J. Allergy Clin. Immunol. 116 (2005) 690–697.

Please cite this article as: K. Maekawa, et al., X-linked agammaglobulinemia in a 10-year-old boy with a novel non-invariant splice-site mutation in *Btk* gene, Blood Cells Mol. Diseases (2010), doi:10.1016/j.bcmd.2010.01.004

International Immunology, Vol. 21, No. 7, pp. 843–858
doi:10.1093/intimm/dxp050

The analysis of the functions of human B and T cells in humanized NOD/shi-scid/γc^{null} (NOG) mice (hu-HSC NOG mice)

Yohei Watanabe[1,2], Takeshi Takahashi[1], Akira Okajima[1], Miho Shiokawa[1], Naoto Ishii[1], Ikumi Katano[3], Ryoji Ito[3], Mamoru Ito[3], Masayoshi Minegishi[4], Naoko Minegishi[5], Shigeru Tsuchiya[2] and **Kazuo Sugamura[1]**

[1]Department of Microbiology and Immunology and [2]Department of Pediatrics, Tohoku University Graduate School of Medicine, 2-1 Seiryo-cho, Aoba-ku, Sendai 980-8575, Japan
[3]Laboratory of Immunology, Central Institute for Experimental Animals, 1430 Nogawa, Miyamae-ku, Kawasaki 216-0001, Japan
[4]Division of Blood Transfusion, Tohoku University Hospital, 2-1 Seiryo-cho, Aoba-ku, Sendai 980-8575, Japan
[5]Department of Health and Welfare Science, Sendai University, 2-2-18 Funaokaminami, Shibata-machi, Miyagi-ken 989-1693, Japan

Keywords: adaptive immunity, humanized mice, NOG mice, thymus

Abstract

'Humanized mice' are anticipated to be a valuable tool for studying the human immune system, but the reconstituted human immune cells have not yet been well characterized. Here, we extensively investigated the differentiation and functions of human B and T cells in a supra-immunodeficient mouse strain, NOD/shi-scid/γc^{null} (NOG) reconstituted with $CD34^+$ hematopoietic stem cells obtained from umbilical cord blood. In these hu-HSC NOG mice, the development of human B cells was partially blocked, and a significant number of B-cell progenitors accumulated in the spleen. The mature $CD19^+IgM^+IgD^+$ human B cells of the hu-HSC NOG mice could produce IgG *in vivo* and *in vitro* by antigenic stimulation. In contrast, although human T cells with an apparently normal phenotype developed, most of them could neither proliferate nor produce IL-2 in response to antigenic stimulation by anti-CD3 and anti-CD28 antibodies *in vitro*. The positive selection of human T cells in the thymus was sufficiently functional, if not complete, and mainly mediated by mouse class II, suggesting that the human T cells lost their function in the periphery. We found that multiple mechanisms were involved in the T-cell abnormalities. Collectively, our results demonstrate that further improvements are necessary before humanized mice with a functional human immune system are achieved.

Introduction

Recently, human immunity research has increased in momentum, owing largely to accumulating evidence that human immunity can be inferred from animal models. However, the extent to which these models directly reflect the human immune system is still open to question. For example, genetic abnormalities often lead to different phenotypes in different species (i.e. patients with spontaneous mutations in a certain gene and the corresponding gene-disrupted mice), resulting in complicated interpretations about the human immune system (1–3). In addition, different responses to pharmacological reagents developed in animals can result in unexpected adverse effects when they are used for therapeutic treatments (4). Hence, the development of novel model systems in which the human immune system can be functionally studied in a reliable manner without various constraints is desired not only for understanding human immunity but also for improving 'translational' research.

'Humanized mice' have been considered one such model (5–9). For the past two decades, many studies have attempted to graft immunodeficient animals with human tissues or cells (10–12). In particular, the inoculation of human hematopoietic cells or PBMCs has been frequently performed to examine whether even a part of the functional human immune system can be reconstituted. Although various immunodeficient mice, including athymic nude mice (*nu/nu*), C.B.-17 *scid* mice, and NOD/SCID mice, have been used as recipients (10–12), there

Correspondence to: T. Takahashi; E-mail: takeshi-takahashi@mail.tains.tohoku.ac.jp
Transmitting editor: K. Yamamoto

Received 13 March 2009, *accepted* 1 May 2009
Advance Access publication 10 June 2009

seem to be major obstacles to the xenotransplantations. For example, the simple transfer of human PBMCs into such immunodeficient animals results in the failure of stable engraftment, the functional impairment of the donor cells and in some cases the uncontrolled activation of human T cells against mouse tissues (xenogenic graft versus host disease) (13, 14). In addition, when human $CD34^+$ hematopoietic stem cells are transferred, the reconstitution of human immune cells is often incomplete, as revealed by a lack of T-cell development in reconstituted NOD/SCID mice (15). Furthermore, the poor graft survival of human hematopoietic stem cells makes it difficult to perform long-term experiments (16). These limitations have hampered the research on human immune systems in humanized mice.

The recent development of a new immunodeficient strain, however, has opened up the possibility for generating better xenotransplantation systems (5, 6, 16). Disruption of the IL-2R γ chain (γc) produces a mouse strain deficient for B, T, NK and NKT cells since the signalings through γc of multiple cytokines (IL-2, IL-4, IL-7, IL-15, etc.) are indispensable for the development of a wide range of immune cell lineages (17–19). By backcrossing the γc knockout (KO) mice onto the NOD background, which has low endogenous NK activity, and introducing the *scid* mutation, the NOD/Shi-scid-IL-2Rγ $(γc)^{null}$ (NOG) strain was generated (16, 20, 21). As a consequence, NOG mice have almost no functional endogenous immune system. Using NOG or the similar BALB-RAG2/γc double-KO mice, several groups have reported a more efficient and stable reconstitution of human hematopoietic cells than was previously possible, using human $CD34^+$ stem cells from various sources, including bone marrow (BM), umbilical cord blood or peripheral blood immobilized by granulocyte colony stimulating factor (16, 20–22). For example, such humanized mice harbor human $CD34^+$ stem cells in their BM for up to 1 year, and the cells can be serially transferred into new recipients to reconstitute them (16). In addition, apparently normal human B and T cells or their progenitors are found in the spleen or BM, respectively (16, 20, 21), and major subsets of human hematopoietic cells have been successfully developed from these mice (22, 23). Hence, these supra-immunodeficient strains are presently considered the most suitable for reconstituting quasi-human immune systems.

Nevertheless, it is also clear that there is room for improvement in the present humanized mouse technology. For example, upon exogenous antigenic challenge, humanized mice (hu-HSC-NOG mice) produce abundant antigen-specific IgM antibodies, but little antigen-specific IgG (21, 22, 24, 25). This predominant IgM production suggests that only a partial reconstitution of the human adaptive immune system is achieved in the hu-HSC-NOG mice. In the present study, we sought to identify critical cues for recapitulating functional human immunity in hu-HSC-NOG mice, mainly focusing on the differentiation and functions of the human B and T cells upon reconstitution.

Methods

$CD34^+$ hematopoietic stem cells

The cord blood from full-term deliveries was obtained from the Miyagi Cord Blood Bank, following the institutional guidelines approved by the Tohoku University Committee on Clinical Investigations. Some $CD34^+$ cell samples were obtained from the RIKEN Bioresource Center Cell Bank (Tsukuba, Japan). Mononuclear cells were isolated from cord blood by density gradient centrifugation using Lymphocyte Separation Medium (MP Biomedicals, Solon, OH, USA) after removing the phagocytes with Silica (Immuno Biological Laboratories, Takasaki, Japan). The cells were washed and suspended in PBS containing 5% FCS. $CD34^+$ stem cells were obtained by magnetic cell sorting (MACS) (Miltenyi Biotech, Bergisch Gladbach, Germany). Briefly, $CD34^+$ cells were labeled with a biotin-conjugated anti-human CD34 mAb (Serotec, Oxford, UK) after FcR blocking and subsequently with anti-biotin microbeads. The magnetically labeled $CD34^+$ cells were purified twice on LS columns. The usual purity of the $CD34^+$ fraction was >95%. The purified $CD34^+$ cells were cryopreserved in Cell Banker (Juji Field, Tokyo, Japan) at −80°C in a deep freezer until use.

Mice and reconstitution with human stem cells

Six-week-old female NOD/shi-scid/$γc^{null}$ (NOG) mice were obtained from the Central Institute for Experimental Animals (CIEA) and maintained in the animal facility of Tohoku University School of Medicine under specific pathogen-free conditions. NOG I-$Aβ^{-/-}$ mice or NOG I-$Aβ^{+/-}$ mice were obtained by backcrossing B6 I-$Aβ^{-/-}$ mice (26) kindly gifted from Mathis and Benoist (Harvard Medical School) onto the NOG background more than five times with a speed congenic technique (27) in CIEA. All the animal experiments were properly conducted according to the institutional guidelines. These mice were irradiated with 120 cGy of X-rays, and 1×10^5 cord blood $CD34^+$ cells, which were resuspended with 200 μl PBS, were transferred into them by intravenous (i.v.) injection later the same day.

Antibodies and flow cytometric analysis

The following mAbs were used. Anti-CD3–FITC, anti-CD4–FITC, anti-CD19–FITC, anti-CD34–FITC, anti-CD45–FITC, anti-CD62L–FITC, anti-CD69–FITC, anti-CD4–phycoerythrin (PE), anti-CD20–PE, anti-CD23–PE, anti-CD44–PE, anti-IgD–PE, anti-CD4–allophycocyanin (APC), anti-CD20–APC, anti-CD28–APC, anti-CD38–APC, ani-IgM–APC, anti-CD11b–APC, anti-CD8–PE–Cy7, anti-CD3–biotin, anti-IgD–biotin and anti-CD132–biotin were purchased from BD PharMingen (San Jose, CA, USA). Anti-CD24–FITC, anti-CD27–PE, anti-CD23–PE, anti-CD10–PE, anti-CD178–PE, anti-CD95–pacific blue, anti-CD19–APC Alexa Fluor 750 and e-Fluor 450 Mouse IgG1, k isotype control were from e-Bioscience (San Diego, CA, USA). Anti-CD5–PE-Cy7 and anti-CD24–PE-Cy5 were from Beckman Coulter (Miami, FL, USA). Anti-CD34–biotin was from Serotec. Anti-TRBV28 (Vβ3)–biotin was from Ancell (Bayport, MN, USA). Biotinylated antibodies were visualized by streptavidin–APC or streptavidin–PE-Cy7 (BD PharMingen). For intracellular staining, anti-human IgM–FITC was purchased from Dako (Glostrup, Denmark). PE-labeled anti-VpreB (HSL96) and $V_{λ5}$ (HSL11) were kindly provided by Karasuyama (28).

To analyze human lymphocytes in the hu-HSC-NOG mice, multicolor cytometric analysis was performed using a FACS

Calibur or FACS Canto II (BD Biosciences). To monitor the reconstitution periodically, peripheral blood was taken from the retro-orbital venous plexus through heparinized pipettes. At the time of sacrifice, single-cell suspensions were prepared from the spleen or BM by mincing with metal mesh or by flushing the tibiae and femurs with PBS containing 2% FCS using a 27-gauge needle. The cells were stained with the relevant mAbs for 15 min on ice, then washed with cold PBS containing 2% FCS and stained with the appropriate secondary antibodies when necessary. We used Cytofix/Cytoperm solution (BD Biosciences) for intracellular staining, according to the manufacturer's instructions. After the final wash, the cells were subjected to flow cytometric analysis. The proportion of each lineage was calculated using CELL Quest or FACS Diva software (BD Biosciences).

ELISA

The concentration of human IgM and IgG in the sera of reconstituted NOG mice was measured using a human Ig assay kit (Bethyl, Denver, CO, USA). For the detection of keyhole limpet hemocyanin (KLH)-specific human IgM and IgG antibodies, humanized NOG mice were immunized two or three times once a week with an emulsion of 500 μg of KLH whole protein (Sigma, St Louis, MO, USA) with CFA (Difco Laboratories, Sparks, MD, USA) in total 100 μl by intra-peritoneal (i.p.) injection. The sera from the immunized mice were harvested 1 week after the final immunization. The specific antibodies against KLH were measured by a standard ELISA. Briefly, 96-well plates were coated with 10 μg ml^{-1} KLH at 4°C overnight. After washing and blocking with PBS containing 1% BSA, the collected serum samples were loaded. HRP-conjugated anti-human Ig antibody was used as a secondary antibody. Both anti-IgG-specific and anti-IgM-specific antibodies were purchased from Bethyl (Montgomery, TX, USA). *o*-Phenylenediamine was used as a substrate for detection. The absorbance at 450 nm was measured by a microplate reader. To detect peptide-specific Ig, we used a peptide-coating kit (Takara, Otsu, Japan), according to the instruction manual.

To detect cytokines in the supernatants, kits for IL-2, IFN-γ or IL-4 (BD Biosciences) were used according to the instruction manuals from the manufacturer.

In vitro cultures

The single-cell suspension of spleen cells from hu-HSC-NOG mice was prepared as described above 16–20 weeks after reconstitution. Human IgD^+ mature B cells were isolated by MACS LS column by using a biotin-conjugated anti-IgD mAb and anti-biotin microbeads. The purity of the isolated fraction was ~90%. The IgD^+ cells were cultured in RPMI medium supplemented with 10% FCS and antibiotics [penicillin G sodium (100 U ml^{-1}) and streptomycin sulfate (100 μg ml^{-1})]. The cells were stimulated with polyclonal anti-IgM antibody at 2 μg ml^{-1} (Jackson Immunoresearch, West Grove, PA. USA) or with *Staphylococcus aureus* cowan (SAC) at 0.01% (Calbiochem, Gibbstown, NJ, USA) in the presence or absence of 1 μg ml^{-1} anti-CD40 antibody (R&D, Minneapolis, MN, USA) with or without a mixture of 100 ng ml^{-1} IL-21 (Peprotech, Rocky Hill, NJ, USA) and 25 U ml^{-1} IL-2 (R&D) in a 96-well plate (2×10^5 in 200 μl per well) for 7 days. The IgM and IgG levels in the culture supernatants were determined by ELISA as described above.

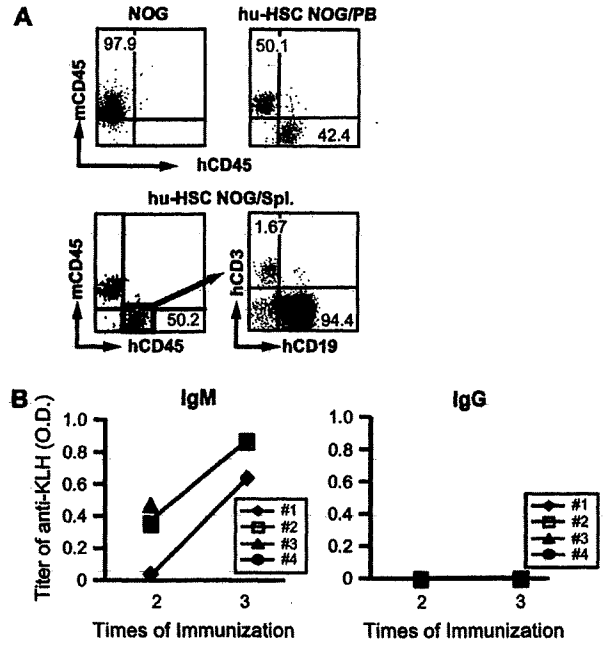

Fig. 1. Reconstitution of NOG mice with human hematopoietic stem cells. (A) Representative FACS analysis of peripheral blood (PB) cells from hu-HSC NOG mice 8 weeks after $CD34^+$ cell transplantation ($n = 6$). Engraftment of human $CD45^+$ ($hCD45^+$) cells in the PB in the hu-HSC NOG is shown (top left panel: control non-transferred NOG mouse, top right panel: hu-HSC NOG). Development of the human $CD19^+$ B cells and $CD3^+$ T cells in the spleen were analyzed in the hu-HSC NOG gated on $hCD45^+$ cells (bottom panels) (8 weeks after reconstitution, $n = 6$). (B) Humoral immune responses in hu-HSC NOG mice. Upon immunization of the hu-HSC NOG mice (at 16weeks after reconstitution, $n = 4$) with KLH/CFA emulsion (500 μg of KLH/CFA, three times), the sera was collected and examined for the presence of KLH-specific human IgM (left panel) or IgG (right panel) by ELISA.

For T-cell stimulation, the total spleen cells of hu-HSC NOG mice were cultured with PHA (1 μg ml^{-1}) or a mixture of soluble anti-CD3 (OKT3, 10 μg ml^{-1}) (BD PharMingen) and anti-CD28 (1 μg ml^{-1}) (Biolegend, San Diego, CA, USA) antibodies in a 96-well round-bottom plate (1×10^5 in 200 μl per well). Human $CD4^+$ or $CD8^+$ T cells in the hu-HSC NOG mice were purified by positive selection by MACS LS column in combination with anti-human CD4 or CD8 microbeads, respectively. The T cells were stimulated with immobilized anti-CD3 (10 μg ml^{-1}) and CD28 (1 μg ml^{-1}) antibodies or mixture of phorbol myristate acetate (50 ng ml^{-1}) and ionomycin (1 μg ml^{-1}) in 96-well round-bottom plates (1×10^5 in 200 μl per well). The T-cell proliferation was measured as the incorporation of [^{3}H]thymidine for the last 6 h of a 72-h culture. Carboxyfluorescein succinimidyl ester (CFSE) labeling was conducted according to a standard protocol.

Reverse transcription–PCR

The expression of mRNA for AID was measured by semi-quantitative reverse transcription (RT)–PCR. The total RNA

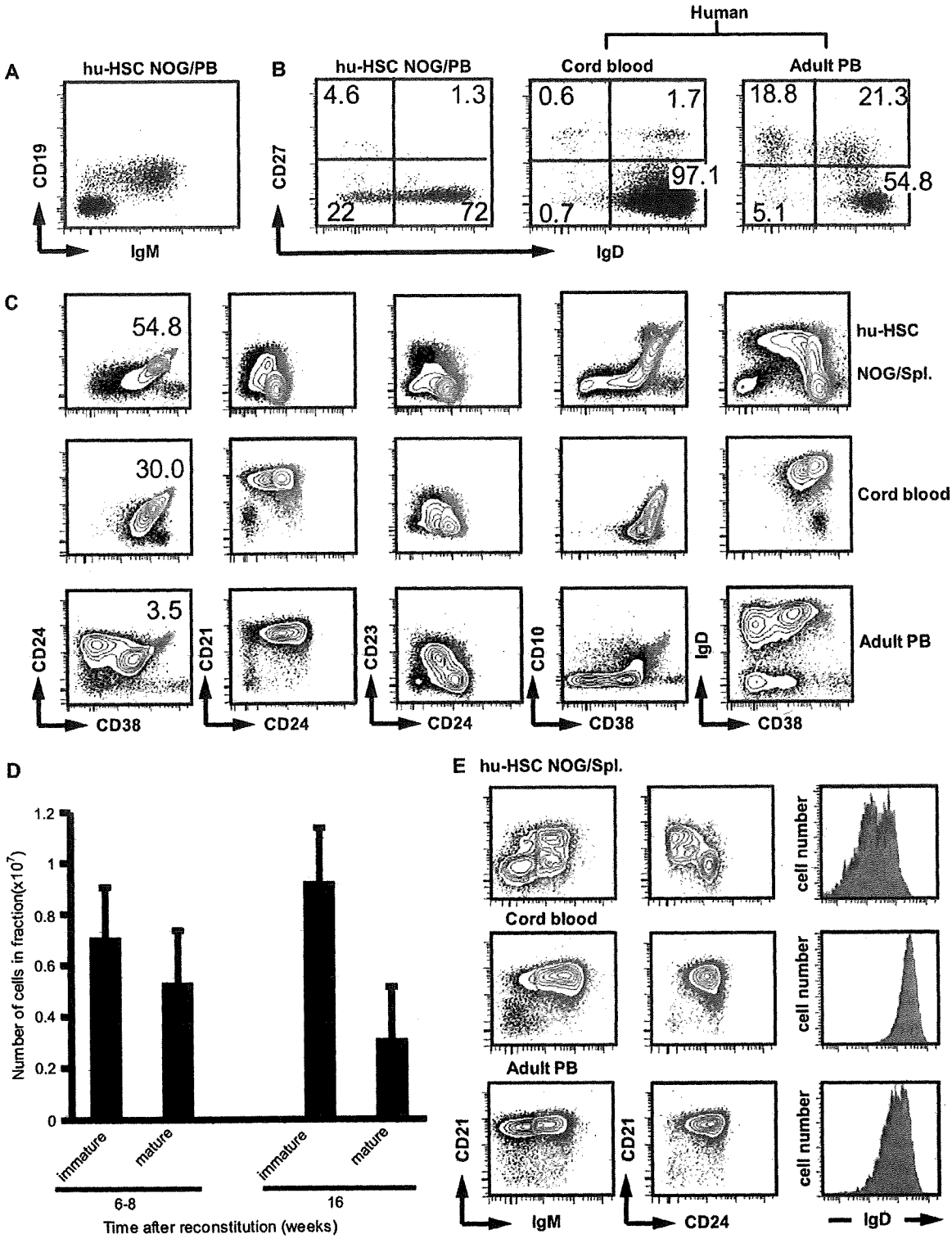

Fig. 2. Analysis of B cells in hu-HSC NOG. (A) Characterization of human B cells in the peripheral blood (PB) of hu-HSC NOG. A representative result of staining with anti-IgM and anti-CD19 antibodies was shown (16 weeks after reconstitution, $n = 6$). (B) Representative staining patterns with anti-IgD and anti-CD27 antibodies are shown gated on $CD19^+$ B cells from various sources [i.e. PB of the hu-HSC NOG (16 weeks after reconstitution, $n = 3$), human cord blood or PB of a normal healthy adult]. (C) A representative analysis of splenic $CD19^+$ cells in hu-HSC NOG by various differentiation-related markers. The whole-spleen cells of the hu-HSC NOG mice (8 weeks after reconstitution, $n = 4$), cord blood-derived

was prepared from cells using Trizol Reagent (Invitrogen, Carlsbad, CA, USA). The concentration of the total RNA was measured by NanoDrop 1000 (Nanodrop Technologies), and the first-strand cDNA was synthesized using SuperscriptIII (Invitrogen) with an oligo (dT) 20 primer. The cDNA for AID, RAG1, RAG2, TdT or glyceraldehyde 3-phosphate dehydrogenase (GAPDH) was amplified with specific primers using Ex-Taq polymerase (Takara). The primer sets were as follows—AID: forward, 5′-gaggcaagaagacactctgg and reverse, 5′-caaaaggatgcgccgaagctgtctggag; RAG1: forward, 5′-ccagctgtttgcttggccatccgt and reverse, 5′-ttgggatctcatgccttccaagat; RAG2: forward, 5′-atgtccctgcagatggtaaca and reverse, 5′-gcctttgtatgagcaagtagc; TdT: forward, 5′-ccaccaattgctgtacaaaaga and reverse, 5′-tcgttcatcatttaacacagctt; β-actin: forward, 5′-gctcgtcgtcgacaacggctc and reverse, 5′-caaacatgatctgggtcatcttctc and GAPDH: forward, 5′-gaaggtgaaggtcggagtca and reverse, 5′-ttcacacccatgacgaacat.

After denaturing at 94°C for 5 min, the cDNA was amplified by a protocol consisting of 94°C for 30 s, 60°C for 30 s and 72°C for 30 s, for 25 cycles. The PCR products were separated on agarose gels and stained with ethidium bromide.

Retroviral vectors

The retroviral vector, pDΔNsam-IRES-EGFP, based on murine stem cell virus with enhanced green fluorescent protein (EGFP) as a marker under an internal ribosomal entry site (IRES) was kindly provided by Onodera (29). PLAT-F, a package cell line that produces a pseudotype virus with an RD114 envelope, was from Kitamura (30) and used to infect $CD34^+$ stem cells. The human *bcl-2* or *HLA-DRB*0401* genes were inserted into the *Not*I and *Bam*HI sites of the pDΔNsam-IRES-EGFP vector.

B16 T cells specific for an influenza hemagglutinin peptide ($HA_{307–319}$) were kindly provided by Buckner (31). The T-cell receptor (TCR) genes (B16 TCR; *TRAV4* and *TRBV28* based on the International Immunogenetics Information System) were isolated by standard techniques from the B16 T cells and cloned into the retroviral vector. *TRAV4* was inserted into the *Not*I/*Bam*HI sites, while *TRBV28* was inserted into the *Nco*I/*Cla*I sites after removing the EGFP gene. To infect human T cells, retrovirus was prepared in the form of a VSV-pseudotype virus in 293T packaging cells, by plasmid DNA transfection using a standard calcium phosphate protocol. After 72 h, the supernatants were recovered and concentrated by centrifugation at 8700 r.p.m. for 19 h at 4°C.

Gene delivery into $CD34^+$ cells by retrovirus

$CD34^+$ cells isolated from cord blood were cultured in X-VIVO 15 (Cambrex Bioscience, Walkersville, MD, USA), supplemented with 1% human serum albumin (HSA) (Kaketsuken, Kumamoto, Japan) and stimulated with a cytokine cocktail [100 ng ml^{-1} stem cell factor (R&D), 100 ng ml^{-1} Flt-3 ligand (Flt-3L) (R&D), 100 ng ml^{-1} thrombopoietin and 100 ng ml^{-1} IL-6 (Peprotech)] in a 24-well plate (2×10^5 per well) for 48 h. During the priming of the $CD34^+$ cells, non-tissue culture-treated six-well plates (Becton Dickinson) were coated with CH-296 recombinant fibronectin fragment (Retronectin) (20 μg ml^{-1}, Takara). The stimulated $CD34^+$ cells were harvested and placed in the CH-296-coated plates (3×10^5 per well) in the presence of the respective virus supernatant. The supernatants were diluted 1:2 with X-VIVO containing 1% HSA, 10 μg ml^{-1} protamine sulfate and the cytokine mixture described above. The cells were spun at 2000 r.p.m. for 30 min at 37°C. Every 12 h, the medium was replaced with fresh virus supernatant. After 48 h of culture, the frequency of GFP- and CD34-expressing cells was examined. About 5×10^5 to 1×10^6 infected cells were injected i.v. into irradiated NOG mice.

Retroviral infection of human T cells

$CD4^+$ T cells were isolated from the PBMCs of normal healthy donors by MACS, as described above. The infection of T cells by retrovirus for B16 TCR was conducted as previously reported (32). Briefly, purified T cells were stimulated in the presence of recombinant human IL-2 (50 U ml^{-1}) on a 24-well plate that had been previously coated with anti-CD3 antibody (1 μg ml^{-1}), anti-CD28 antibody (1 μg ml^{-1}) and Retronectin (12 μg ml^{-1}). Half of the culture medium was replaced by fresh medium supplemented with IL-2 every 48 h. On days 4 and 5, the T cells were spin-infected with the concentrated virus (2000 r.p.m., 90 min at 32°C). After a further 1 week of culture, the expression of B16 TCR on the T cells was examined by staining with anti-TRBV28 antibody, APC-conjugated HLA-DRB1*0401/$HA_{307–319}$ (PKYVKQNTLKLAT) or HLA-DRB1*0401/human $CLIP_{103–117}$ (PVSKMRMATPLLMQA) tetramers (kindly provided by National Institute of Health tetramer core facility). These T cells (1×10^6 or 3×10^6) were transferred into reconstituted NOG mice by i.v. injection and subsequently i.p. immunized with HA peptide/CFA emulsion (100 μg HA peptide in total 100 μl).

Results

Reconstitution of NOG mice with human $CD34^+$ stem cells

In the fully reconstituted NOG mice, a significant amount of human B and T cells appeared in the peripheral blood and comprised major fractions in the spleen, as previously reported (16) (Fig. 1A). Immunization of the hu-HSC NOG mice with a protein antigen, KLH, with CFA evoked an antigen-specific IgM response, but a negligible antigen-specific IgG response (Fig. 1B). This finding was also consistent with previous reports (21, 22, 24, 25).

Analysis of the human B cells in hu-HSC NOG mice: partial differentiation of the human B cells

To elucidate the mechanisms for the poor IgG response in the hu-HSC NOG mice, we analyzed the development and

cells or PB from a normal adult were stained with respective antibodies. $CD24^{int/hi}CD38^{hi}$ immature population is highlighted by red contour plot. (D) The number of immature ($CD19^+CD24^{int/hi}CD38^{hi}$) or mature ($CD19^+CD24^{lo}CD38^{lo}$) B cells from hu-HSC NOG at different time points after reconstitution. The means of the cell number of each B-cell population are represented with standard deviation ($n = 3$ for each group). (E) Partial differentiation of human B cells in the spleen in hu-HSC NOG mice. The expression patterns of CD24, CD21 or IgD on $CD19^+IgM^+$ B cells (highlighted by blue contour plot) from the hu-HSC NOG mice (8 weeks after reconstitution, $n = 4$), cord blood or adult PB are shown.